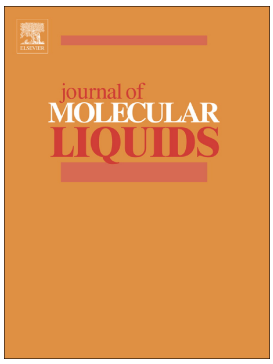

Entropy generation of nanofluid and hybrid nanofluid flow in thermal systems: A review

Gabriela Huminic, Angel Huminic

PII: S0167-7322(19)36897-7

DOI: https://doi.org/10.1016/j.molliq.2020.112533

Reference: MOLLIQ 112533

To appear in: *Journal of Molecular Liquids*

Received date: 16 December 2019

Accepted date: 18 January 2020

Please cite this article as: G. Huminic and A. Huminic, Entropy generation of nanofluid and hybrid nanofluid flow in thermal systems: A review, *Journal of Molecular Liquids*(2020), https://doi.org/10.1016/j.molliq.2020.112533

Entropy generation of nanofluid and hybrid nanofluid flow in thermal systems: A review

Gabriela HUMINIC[1*], Angel HUMINIC[1]

[1]Transilvania University of Brasov, Mechanical Engineering Department

29, Bulevardul Eroilor, 500036 Brasov, Romania

* Corresponding Author: Gabriela HUMINIC: e-mail: gabi.p@unitbv.ro; tel. +040268474761

Abstract:

This paper presents a review of the contributions on entropy generation of nanofluids and hybrid nanofluids in the different types of thermal systems for different boundary conditions and physical situations. The relevant papers are classified into three categories: entropy generation in minichannel, entropy generation macrochannel and entropy generation in cavities. The viscous dissipative, streamwise, electromagnetic effects, as well as nanoparticles concentration, the temperature and the flow regime on entropy generation, were analyzed. The reviewed literature indicates that the implementation of nanofluids/hybrid nanofluids in microchannels, minichannels, and cavities may be an important alternative to the traditional thermal systems and an interesting topic of study.

Keywords: entropy generation, nanofluid, hybrid nanofluid, microchannel, minichannel, cavity

Nomenclature

Bi	Biot number
Br'	modified Brinkman number
c_p	specific heat at constant pressure, in J/kgK
d_p	particle diameter, in m
D	inner diameter of microchannel, in m
Da	Darcy number
$D_{\square}$	hydraulic diameter, in m
Ec	Eckert number
f	friction factor
Ha	Hartmann number
k	thermal conductivity, in W/m K
L	length of the microchannel, in m
$\dot{m}$	mass flow rate, kg/s
Nu	Nusselt number
Pe	Peclet number
Pr	Prandtl number
q'	heat flux per unit length, W/m
q''	heat flux, in W/m^2
q''_w	wall heat flux, in W/m^2
q'''_{gen}	solid-phase volumetric heat generation, in

Greek symbols

ε	porosity coefficient
θ	dimensionless temperature
μ	effective dynamic viscosity, in $Pa \cdot s$
ν	kinematic viscosity, m^2/s
ρ	fluid density, in kg/m^3
ϕ	nanoparticle concentration, in %
Φ	viscous dissipation function

Subscript

f	base fluid
NF	nanofluid
p	nanoparticles

	W/m^3
R	dimensionless radial coordinate
Re	Reynolds number
r_0	internal radius of microchannel, in m
T	temperature, in K
T_w	wall temperature, in K
u	fluid velocity, in m/s
$\bar{u}$	mean velocity of fluid, in m/s;

Contents

1. Introduction

Micro/nano heat transfer has been an important issue for researchers in the last decades. The microdevices (devices with dimensions between 1 μm and 1 mm) are successfully employed in a variety of fields such as electronics, aerospace, telecommunication, biomedical and automotive industries to enhance heat transfer for heating and cooling. The heat transfer efficiency can be improved by several methods, such as the use of extended surfaces, the application of vibration to heat transfer surfaces, and the use of mini/microchannels. Also, heat transfer efficiency of the microdevices can also be improved by enhanced thermo-physical properties of the working fluid, especially the thermal conductivity and the specific heat [1]. The working fluids with the thermo-physical properties improved are called nanofluid/hybrid nanofluid. By combining nanofluid/hybrid nanofluid with the small channel's dimensions of the thermal devices, it is to obtain devices that provide compactness, low thermal resistance and efficiency.

The entropy generation analysis is a useful tool for performance optimization of the thermal systems. It is known as the addition of nanoparticles into the base fluid could be influence the total entropy generation. Thus, the use the nanofluids in the thermal systems decrease the temperature of the system and finally the heat transfer contribution to the total entropy generation rate decreases, while nanoparticles added into the base fluid increase the viscosity of the working fluid leads to increase pressure drop in the system. Many researchers have studied the entropy generation in order to find optimum conditions for different thermal systems and only a few reviews have been devoted to this topic. For example, Sciacovelli et al. [2] conducted a review of contributions to the theory and application of entropy generation analysis to different engineering systems, while Manjunath and Kaushik [3] analyzed the studies based on second law

analysis applied to heat exchangers. Later, Torabi et al. [4] conducted a state of the art on the entropy generation modeling in porous systems. Regarding the entropy generation in nanofluid/hybrid nanofluid flow only a review was carried out (Mahian et al. [5]). This review provides a comprehensive analysis on entropy generation in different geometries and flow regimes.

This paper aims to providing a comprehensive review on the entropy generation in thermal systems using nanofluids/hybrid nanofluids. Thus, the research conducted regarding the use of the nanofluids/hybrid nanofluids in different channels (microchannel, minichannel, cavities and enclosure) has also been reported and comprehensively analyzed.

2. Entropy generation due to nanofluid flow and heat transfer

In the following an analysis of the investigations carried out on entropy generation in different types of channels in which nanofluids/hybrid nanofluids have been employed is presented. An important difference between macrochannels and microchannels is the hydraulic diameter. A classification of the micro/nanodevices for single and two-phase applications in the function of the hydraulic diameter was proposed by Kandlikar and Grande [6]:

Conventionnel Channels	$D_h > 3\ mm$
Minichannels	3 mm ≥ D_h > 200 μm
Microchannels	200 μm ≥ D_h > 10 μm
Transitional Channels	10 μm ≥ D_h > 0.1 μm
Transitional	10 μm ≥ D_h > 1 μm

Microchannels:

Transitional Nanochannels: 1 μm ≥ D_h > 0.1 μm

Molecular Nanochannels: $D_h \leq$ 0.1 μm

2.1.Entropy generation in microchannels

The development of the microchannels in the last decades encouraged their use in various applications as in the automotive, refrigeration and aerospace industries, where minimization of space and weight of heat exchangers has always been a challenge. The forms of entropy generation in microchannels are attributed to the heat transfer and the fluid friction irreversibilities. First studies on entropy generation in microchannels using nanofluids were carried out by Singh et al. [7] and Mah et al. [8]. Singh et al. [7] theoretical investigated the entropy generation in three different channels (microchannel ($D_{\square} = 0.1\,mm$), minichannel ($D_{\square} = 1.0\,mm$) and conventional channel ($D_{\square} = 10\,mm$) using Al_2O_3/water nanofluids in laminar and turbulent regimes.

Starting to the equation of the rate of entropy generation per unit length for forced convection through a tube with the diameter *D* and the wall heat transfer per unit length q' proposed by Bejan [9],

$$\dot{S}'_{gen} = \frac{1}{\pi\, Nu}\frac{q'^2}{k\,T^2} + \frac{\dot{m}^3\, f}{\rho^2\, T\, r_0^5} = \frac{q'^2}{\pi\, k\, T^2\, Nu\, (Re_D \mathrm{Pr})} + \frac{32\,\dot{m}^3\, f(Re_D)}{\pi^2 \rho^2\, T\, D^5} \quad (1)$$

Singh et al. [7] proposed two equations for the ratio of entropy generation due to nanofluid flow to the base fluid in both laminar and turbulent flows:

- Laminar flow: $Nu = 48/11$ and $f = 64/Re$

$$\frac{\dot{S}'_{gen,NF}}{\dot{S}'_{gen}} = \frac{k}{k_{NF}} \frac{\rho^2}{\rho_{NF}^2} \frac{T^2}{T_{NF}^2} \left(\frac{C_{1l,NF}\ \rho_{NF}^2 + C_{2l,NF}\ \mu_{NF}\ k_{NF}\ T_{NF}}{C_{1l}\ \rho^2 + C_{2l}\ \mu\ k\ T} \right) \tag{2}$$

where the constants C_{1l} and C_{2l} are defined as

$$C_{1l} = \frac{11}{48}\ q''^2\ \pi\ D^2 \text{ and } C_{2l} = \frac{128\ \dot{m}^2}{\pi\ D^4} \tag{3}$$

and q'' is heat flux per unit length (W/m).

- Turbulent flow: $Nu = 0.023\ Re^{0.8}\ Pr^{0.4}$ (Dittus–Boelter and Blasius equations) and $f = 0.316\ Re^{-1/4}$

$$\frac{\dot{S}'_{gen,NF}}{\dot{S}'_{gen}} = \frac{k^{0.6}}{k_{NF}^{0.6}} \frac{\rho^2}{\rho_{NF}^2} \frac{T^2}{T_{NF}^2} \frac{\mu_{NF}^{0.25}}{\mu^{0.25}} \frac{c_p^{0.4}}{c_{p,NF}^{0.4}} \left(\frac{C_{1t,NF}\ \rho_{NF}^2\ \mu_{NF}^{0.15} + C_{2t,NF}\ k_{NF}^{0.6}\ c_p^{0.4}\ T_{NF}}{C_{1t}\ \rho^2 \mu^{0.15} + C_{2t}\ k^{0.6}\ c_p^{0.4}\ T} \right) \tag{4}$$

where:

$$C_{1t} = \frac{43.478}{\left(\frac{4\ \dot{m}}{\pi\ D}\right)^{0.8}}\ q''^2\ \pi\ D^2 \text{ and } C_{2t} = \frac{10.112\ \dot{m}^3}{\pi^2\ D^5} \left(\frac{4\ \dot{m}}{\pi\ D}\right)^{-1/4} \tag{5}$$

It should be noted that in Ref. [7], in Eq. (1), the friction factor, *f*, is multiplied by 8 instead of 32.

Their results showed that the use of Al_2O_3–water nanofluid is beneficial in microchannels in turbulent flow and in conventional channel under laminar flow respectively. They concluded also that there is an optimum diameter at which the entropy generation is the minimum.

Ebrahimi et al. [10] numerical investigated the entropy generation in a rectangular microchannel with longitudinal vortex generators (LVGs) using Al_2O_3 and CuO nanoparticles with different volume concentrations (0.5%-3.0%) and particle sizes dispersed in pure water. The microchannel

is heated by a constant heat flux ($20\ W/m^2$) and has a hydraulic diameter of *160 μm* and *6* pairs of LVGs.

In this study, the dimensionless total entropy generation is defined as:

$$\dot{S}_n = \dot{S}_{n,FF} + \dot{S}_{n,HT} = \underbrace{\frac{\mu}{T}\left(\frac{\partial u_i}{\partial x_j} + \frac{\partial u_j}{\partial x_i}\right)\frac{\partial u_i}{\partial x_j}\frac{k\,T_{in}^2}{q"_w^2}}_{S_{n,FF}} + \underbrace{\frac{k}{T^2}\left[\left(\frac{\partial T}{\partial x}\right)^2 + \left(\frac{\partial T}{\partial y}\right)^2 + \left(\frac{\partial T}{\partial z}\right)^2\right]\frac{k\,T_{in}^2}{q"_w^2}}_{S_{n,HT}} \quad (6)$$

They evaluated the thermodynamic gain using nanofluids as coolant and found that using nanofluids causes a reduction in entropy generation in microchannels with LVGs compared to pure water (Fig. 1). As can be seen from this figure, larger Al_2O_3 ($d_p = 47.0\ nm, \phi = 3.0\%$) and smaller CuO ($d_p = 29.0\ nm, \phi = 1.0\%$)) nanoparticles cause higher irreversibility in the system. Also, they noted that there is not a minimum value for total entropy generation for all parameters studied.

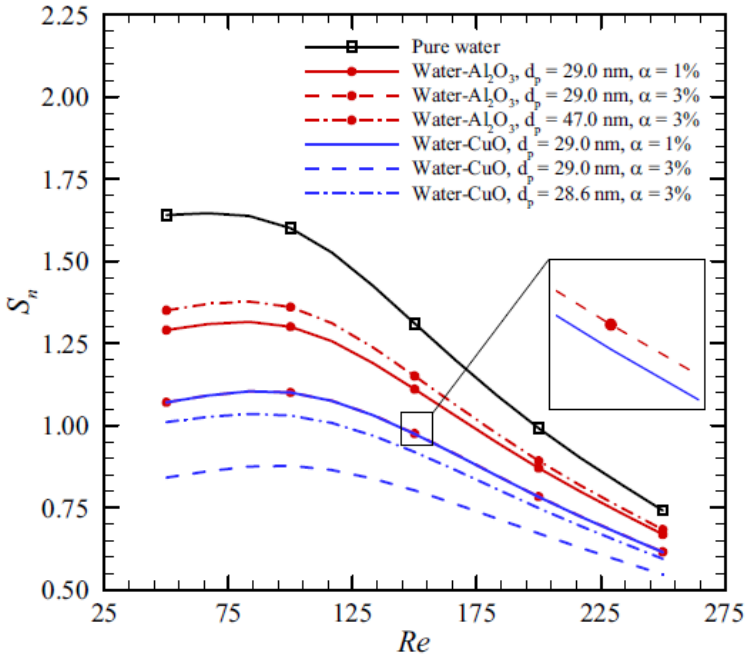

Fig. 1. The dimensionless entropy generation as a function of Reynolds number for nanofluids containing Al_2O_3 or CuO nanoparticles of different sizes with various concentrations [10]. Reprinted with permission from Elsevier.

The theoretical and numerical investigations on the entropy generation in parallel microchannel cooling systems (PMCS) were carried out by Maganti and Dhar [11]. In this study, Al_2O_3/water nanofluid with different volume concentrations and PMCS of three different configurations, U, I and Z, have been studied. The Eulerian–Lagrangian discrete phase approach (DPM) and the conventional effective property approach (EPM) have been used for nanofluid modeling.

The entropy generation rate is calculated as:

$$\dot{S}_{gen} = \underbrace{\frac{q''^2 \pi D^2}{k T^2 Nu((Re)_D, Pr)}}_{(\dot{S}_{gen})_{HT}} + \underbrace{\frac{8 \dot{m}^3}{\pi^2 \rho^2 T} \frac{f((Re)_D)}{D^5}}_{(\dot{S}_{gen})_{FF}} \tag{7}$$

Their results showed that for a nanoparticle concentration, a flow configuration or a Reynolds number given, the entropy generation rate is different when nanofluid flow is modeled using two different models (DPM and EPM). EPM model appreciably higher entropy generation rate compared to the DPM model, because in the case of EPM model, nanofluid is modeled based on the continuum approach (the effective viscosity is considered throughout the fluid), while in the DPM model, the nanofluid is considered to be a two components fluid and the effect of nanoparticles in the flow field is determined based on a Lagrangian path line approach. They also studied the behavior of the adiabatic and diabatic components of entropy generation as a function of Reynolds number using EPM and DPM models and found that for the adiabatic case, it can be noticed that nanofluids lead to higher entropy generation rates which steeply increases with Re, while the diabatic component of entropy generation follows a completely different trend (Fig.2).

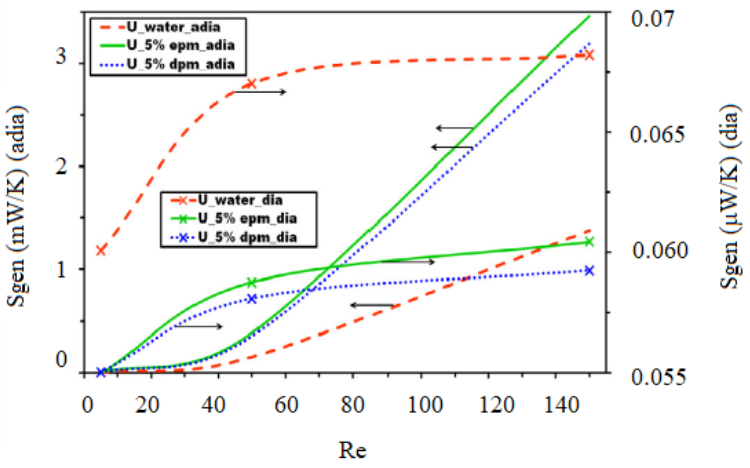

Fig. 2. Individual behaviour of the adiabatic (friction) and the diabatic (heat transfer) components of entropy generation in case of water and nanofluids (both EPM and DPM) with Re [11]. Reprinted with permission from Elsevier.

Heshmatian and Bahiraei [12] numerical studied the entropy generation due to irreversibilities caused by the heat transfer and the fluid friction considering nanoparticle migration in terms of nanoparticle size, wall heat flux, and nanoparticles concentration for the TiO_2/ water nanofluid flow in a circular microchannel. The effects of viscosity gradient, non-uniform shear rate and Brownian diffusion on particle migration were studied. To modeling the total, frictional and thermal entropy generation rates of the nanofluid flow, the multilayer perceptron (ANN) is employed. They noticed that the particle migration intensifies with the increasing of the particles size and their mean concentration. In additional, the total entropy generation rate decreases with the increasing of the particle size due to the friction, which is the main cause of the entropy generation in the microchannel.

Yang et al. [13] numerical investigated the effects of the ratio of upper width and lower width of the microchannel, ratio of the height of the microchannel to the difference between the upper and

lower width of the microchannel, as well as the effect of the volume concentrations of nanoparticles on entropy generation in a trapezoidal microchannel using nanofluids. Numerical analyzes were performed under the following conditions: the hydraulic diameter, $D_{\square} = 106.66\,\mu m$, the inlet velocities, $w = 4\,m/s$, $w = 6\,m/s$, $w = 10\,m/s$, and the heat flux $q" = 200\,kW/m^2$. They found that the highest thermal entropy generation was obtained near bottom and side walls because the difference between temperatures of the fluid and wall was significant, the effect thermal entropy being approximately three times higher than frictional effect.

In another study, Mohammadian et al. [14] numerical studied the entropy generation in a counter flow microchannel heat exchanger (CFMCHE) with two different working fluids in hot and cold channels (water and Al_2O_3/water nanofluid). The simulations were performed under the following conditions: the volume concentrations between 1.0–4.0%, the nanoparticles diameters, 29, 38.4, and 47 nm, and Reynolds number within the range 120 – 480. The results showed that the frictional contribution of entropy generation increases with decreasing particles size and increasing volume concentration, while the trends for heat transfer contribution of entropy generation are opposite. Total entropy generation decreases with decreasing particles size and increasing volume fraction, the maximum performance being occurred at lower particles sizes and higher volume concentrations.

Sohel et al. [15] analytical studied the entropy generation in a circular microchannel and minichannel heat sink using two types of nanoparticles (Cu and Al_2O_3) and two types of base fluids (water and ethylene glycol) respectively, in turbulent flow. They concluded that the

entropy generation decreased by the increasing of volume concentration of both types of nanoparticles dispersed in water and ethylene glycol and also that the entropy generation rate ratio in microchannel was lower than the unity and it decreased by the increasing of volume fraction, while the entropy generation rate ratio in minichannel was higher than the unity for both Al_2O_3/water and Al_2O_3/EG nanofluids. Thus, for microchannel, at a concentration of 6.0 %, the maximum decreasing rate in entropy generation rate ratio was 36% using Cu/H_2O nanofluid and 16% for Al_2O_3/H_2O nanofluid, while for the EG base fluid decreasing rate in the entropy generation rate ratio was 34% and 14% using Cu/EG and Al_2O_3/EG nanofluid respectively. For minichannel, the maximum reductions in the entropy generation rate ratio were 41% and 38% using Cu/H_2O and Cu/EG nanofluid respectively, at the same nanoparticles concentration.

The effects of volume concentration of nanoparticles and microchannel heights on entropy generation of TiO_2-water nanofluid in microchannel heat sink under laminar flow were experimental investigated by Manay et al. [16]. Different microchannel heights (200 mm, 300 mm, 400 mm and 500 mm) and different volume concentrations of nanoparticles (0.25%, 0.5%, 1.0%, 1.5% and 2.0% were analyzed. They found that reducing the height of the microchannel the total entropy generation remarkably increases. Thus, the total entropy generation at $H = 200\ \mu m$ was higher nearly 100 times than that at a $H = 500\ \mu m$ (Fig. 3). Also, the increase of volume concentration leads to increasing entropy generation number ratio. By adding TiO_2 nanoparticles the thermal entropy generation decreases from 32.4% to 1.8% and the frictional entropy generation increases from 3.3% to 21.6%. Following the experiments carried out it can be concluded that the cases of $H = 500\ \mu m$ and $Re \leq 450$ were found to be advantageous from thermodynamically point of view.

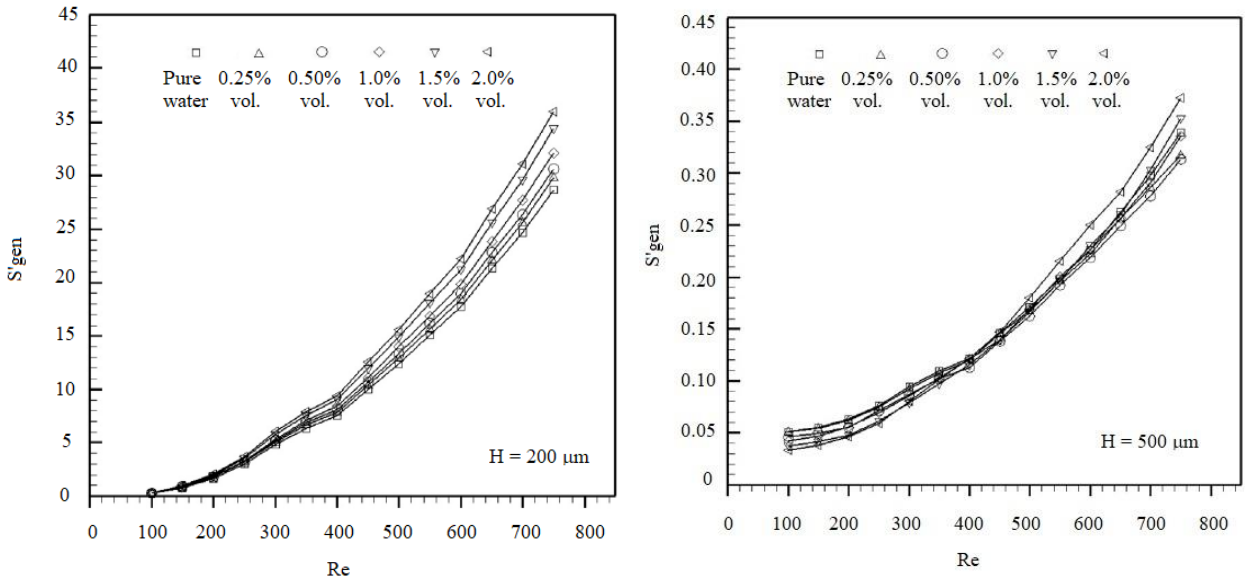

Fig. 3. Total entropy generation rates for (a) H = 200 μm and (b) H = 500 μm [16].

Alfaryjat et al. [17] numerical investigated the effects of the different heat fluxes ($125, 200,$ and $500\ kW/m^2$), Reynolds numbers (200 and 1500), volume fractions (1%, 2.5% and 4%) and different nanoparticle sizes (25, 44, 55 and 70 nm) on the entropy generation for different types of nanofluids (Al_2O_3/water, CuO/water and SiO_2/water) in a hexagon microchannel heat sink (HMCHS). They found that the increase in the heat flux leads to an increase in total entropy generation for different types of nanofluids and water and also that the total entropy generation for any volume concentration and nanoparticle size increases with increasing the heat flux.

Al-Rashed et al. [18] numerical studied the entropy generation of a non-Newtonian nanofluid containing CuO nanoparticles in an offset strip-fin microchannel heat sink (MCHS). The results showed that by increasing of the Reynolds number from 100 to 300, the global total entropy

generation rate significant decreases, while increasing the Reynolds number ($Re > 300$) leads to increasing the global total entropy generation rate.

2.1.2. Viscous dissipative effect

The effect of the viscous dissipative on entropy generation in circular microchannels using Al_2O_3-water nanofluid under laminar flow was analytical studied by Mah et al. [8]. Two mathematical models with and without viscous dissipative term in the energy equation were developed:

Model 1 (with viscous dissipation):

The dimensionless entropy generation is the sum between the dimensionless entropy generation due to the conductive heat transfer in radial and axial directions (N_{HT1}) and the dimensionless entropy generation due to the fluid friction (N_{FF1}):

$$
\begin{aligned}
N_{S1} = \frac{\dot{S}'''_{gen}\, r_0^2}{k_{eff}} = N_{HT1} + N_{FF1} &= \underbrace{\left(\frac{\psi}{1+\psi\,\theta_1}\right)^2 \left[\left(\frac{d\theta_1}{dR}\right)^2 + 4\left(\frac{1+8\,Br'}{Re\,Pr}\right)^2\right]}_{N_{HT1}} + \underbrace{\frac{Br'\left(\frac{\psi}{1+\psi\,\theta_1}\right)\left(\frac{d\widehat{u}}{dR}\right)^2}{}}_{N_{FF1}} \\
&= \underbrace{16\frac{\{(16\,Br'+1)^2\,R^6 - 4(16\,Br'+1)(8\,Br"+1\,)\,R^4 + 4(8\,Br'+1)^2\,R^2 + 16(8\,Br'+1)^2/(Re\,Pr)^2\,\}}{\left[(16\,Br'+1)\,R^4 - 4(8\,Br'+1)\,R^2 + 16\,Br' - \frac{8}{\psi} + 3\right]^2}}_{N_{HF1}} \\
&\quad \underbrace{- \frac{128\,Br'R^2}{\left[(16\,Br'+1)\,R^4 - 4(8\,Br'+1)\,R^2 + 16\,Br' - \frac{8}{\psi} + 3\right]}}_{N_{FF1}} \\
&= 16\left\{(16\,Br'+1)(8\,Br'+1)\,R^6 - 4(8\,Br'+1)^2\,R^4 + 4\left[32\,Br' + 2\,Br'\left(\frac{8}{\psi}+5\right)+1\right]R^2\right. \\
&\quad \left. + 16(8\,Br'+1)^2/(Re\,Pr)^2\right\} \Big/ \left[(16\,Br'+1)\,R^4 - 4(8\,Br'+1)\,R^2 + 16\,Br' - \frac{8}{\psi} + 3\right]^2
\end{aligned}
\tag{8}
$$

In Equation (6):

- $\dot{S}'''_{gen}$ is the volumetric rate of entropy generation (in $W/m^3\,K$):

$$\dot{S}'''_{gen} = \dot{S}'''_{HT} + \dot{S}'''_{FF} = \frac{k_{eff}}{T^2}(\nabla T)^2 + \frac{\mu_{eff}}{T}\,\Phi = \frac{k_{eff}}{T^2}\left[\left(\frac{\partial T}{\partial x}\right)^2 + \left(\frac{\partial T}{\partial r}\right)^2\right] + \frac{\mu_{eff}}{T}\left(\frac{\partial u}{\partial r}\right)^2 \tag{9}$$

- ψ is the dimensionless heat flux:

$$\psi = \frac{q_w\, D}{k_{eff}\, T_w} \tag{10}$$

- θ_1 is the dimensionless temperature profile:

$$\theta_1(R) = -\frac{1}{8}(1 + 16\,Br')R^4 + \frac{1}{2}(1 + 8\,Br')\,R^2 - \frac{3}{8}\left(1 + \frac{16}{3}\,Br'\right) \tag{11}$$

- Br' is the Brinkman number based on uniform heat flux condition:

$$Br' = \frac{\mu_{eff}\,\bar{u}^2}{q_w\, D} \tag{12}$$

Model 2 (without viscous dissipation):

$$\begin{aligned} N_{S2} = N_{HT2} + N_{FF2} &= \underbrace{\left(\frac{\psi}{1+\psi\,\theta_2}\right)^2\left[\left(\frac{d\theta_2}{dR}\right)^2 + \frac{4}{(Re\,Pr)^2}\right]}_{N_{HT2}} + \underbrace{Br'\frac{\left(\frac{\psi}{1+\psi\,\theta_2}\right)\left(\frac{d\hat{u}}{dR}\right)^2}{}}_{N_{FF2}} \\ &= \underbrace{\frac{16\left[R^6 - 4\,R^4 + 4\,R^2 + \frac{16}{(Re\,Pr)^2}\right]}{\left(R^4 - 4\,R^2 - \frac{8}{\psi} + 3\right)^2}}_{N_{HT2}} - \underbrace{\frac{128\,Br'R^2}{R^4 - 4\,R^2 - \frac{8}{\psi} + 3}}_{N_{FF2}} \\ &= 16\left\{(1 - 8\,Br')\,R^6 + 4(8\,Br' + 1)\,R^4 + 4\left[2\,Br'\left(\frac{8}{\psi} - 3\right) + 1\right]R^2 + 16/(Re\,Pr)^2\right\} \\ &\quad /(R^4 - 4\,R^2 + 3 - 8/\psi)^2 \end{aligned} \tag{13}$$

where the dimensionless temperature profile, $\theta_2(R)$is given by:

$$\theta_2(R) = -\frac{1}{8}R^4 + \frac{1}{2}\,R^2 - \frac{3}{8} \tag{14}$$

The results showed that if the viscous effect is considered the entropy generation increases with the increase in volume concentration of nanoparticles. This is due to the increase the thermal conductivity and viscosity of Al_2O_3-water nanofluid which causes rising in the heat transfer and fluid friction irreversibilities.

Ting et al. [19] investigated the entropy generation of viscous dissipative Al_2O_3/water nanofluids flow in asymmetrically heated porous microchannels with solid-phase heat generation. They found that, in absence solid-phase heat generation, the entropy generation is minimum, if the walls are heated symmetrically (at a wall heat flux ratio $\Omega_w = 0.5$), thus achieving a reduction in entropy generation of approximately 17%. If the solid-phase heat generation is considered, then the entropy generation is minimum at a wall heat flux ratio of 3/4 ($\Omega_w = 0.75$). For the first case (without solid-phase heat generation), the entropy generation is minimum at $Re_{opt} = 22$, while for the second case, there is no an optimum Reynolds number due to the domination of solid-phase heat generation irreversibility over the other irreversibilities. They concluded that the effect of thermal asymmetry different influence the entropy generation in the case with and without solid-phase heat generation (Fig. 4).

Case 1: Without solid-phase heat generation

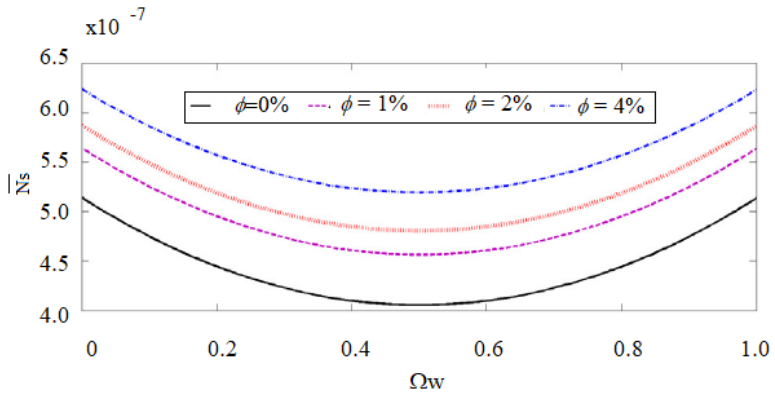

a)

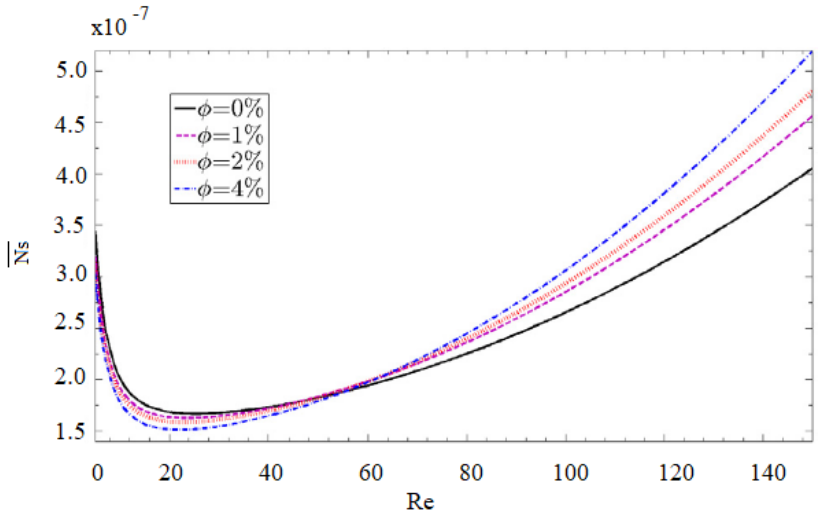

b)

Case 2: With solid-phase heat generation

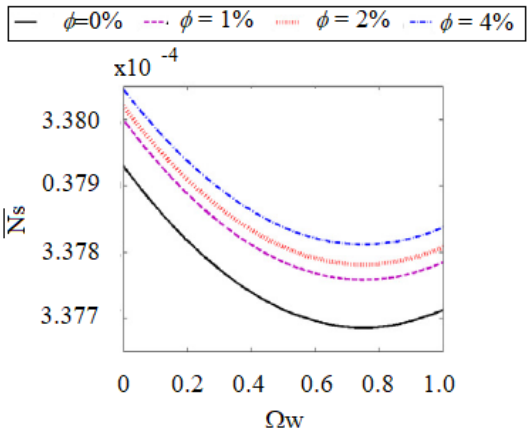

c)

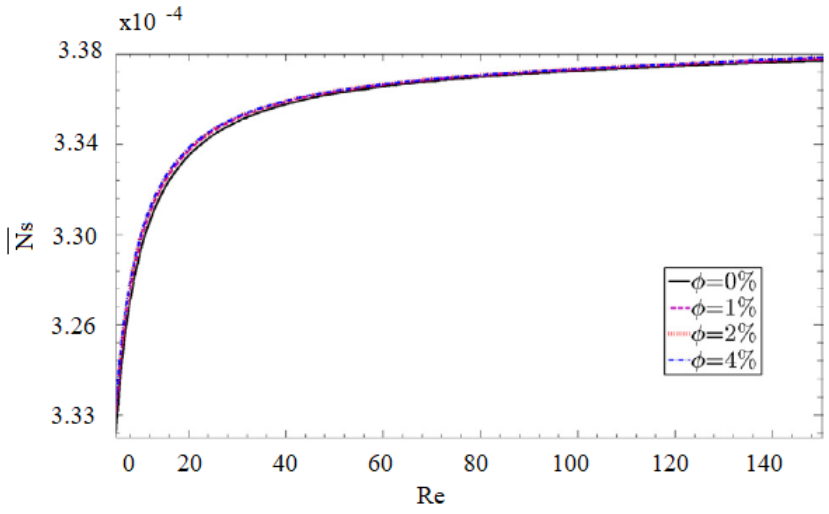

d)

Fig. 4. The total entropy generation versus the wall heat flux ratio, Ω_w, and Reynolds number, Re [19]. Reprinted with permission from Elsevier.

2.1.3. Streamwise effect

Because the effect of the streamwise conduction was neglected due to the low thermal conductivity of conventional fluids, the development of advanced working fluids (nanofluids) has led to intensify those researches on this topic. Thus, the effects of streamwise conduction, nanoparticle concentration and microchannel aspect ratio on the entropy generation of Al_2O_3-water nanofluid flow in circular microchannel heat sinks was analytical investigated by Ting et al. [20]. Two mathematical models with and without streamwise conduction term in the energy equation were developed:

Model 1 (with the streamwise conduction):

The dimensionless entropy generation is given by:

$$N_{S1} = N_{HT1} + N_{FF1} = \underbrace{\left[\frac{\varpi\ \xi}{2\left(\varpi\ \bar{\theta}_1 + \frac{1}{C_k}\right)}\frac{\partial\bar{\theta}_1}{\partial X}\right]^2}_{N_{HT1}} + \underbrace{\frac{C_\mu \varpi\ Br'}{C_\mu \varpi\ \bar{\theta}_1 + 1}\left(\frac{\partial U}{\partial R}\right)^2}_{N_{FF1}}$$

$$= \Big\{C_a\ C_k\ \xi\ \hat{\beta}\ \varpi\ \Big[C_a\ C_b\left(exp(C_a\ X - C_a - \hat{\beta}) - exp(-\hat{\beta}\ X)\right) + C_a\ C_c(exp(C_a\ X - C_a) - 1) + C_c\ \hat{\beta}\ (exp(C_a\ X - C_a) - 1)\Big]\Big\}^2$$

$$/\Big\{4\{C_a\ C_b\ C_k\ \varpi[C_a + \hat{\beta}\ exp(-C_a - \hat{\beta}) - C_a\ exp(-\hat{\beta}\ X) - \hat{\beta}\ exp(C_a\ X - C_a - \hat{\beta})] + C_a\ C_c\ C_k\ \hat{\beta}\ \varpi[C_a\ X + \hat{\beta}\ X + exp(-C_a) - exp(C_a\ X - C_a) - C_c\ C_k\ \hat{\beta}^2\ \varpi\ [exp(C_a\ X - C_a) - exp(-C_a)] + C_a\ \hat{\beta}\ (C_a + \hat{\beta})]\}^2\Big\} + \quad (15)$$

$$+\left[16\ R^2\ C_a^2\ \hat{\beta}\ \varpi\ Br'(C_a + \hat{\beta})\right]$$

$$/\{C_a\ C_b\ C_k\ \varpi[C_a + \hat{\beta}\ exp(-C_a - \hat{\beta}) - C_a exp(-\hat{\beta}\ X) - \hat{\beta}\ exp(C_a\ X - C_a - \hat{\beta})]$$

$$+ C_a\ C_c\ C_k\ \hat{\beta}\ \varpi[C_a\ X + \hat{\beta}\ X + exp(-C_a) - exp(C_a\ X - C_a)]$$

$$- C_c\ C_k\ \hat{\beta}^2\ \varpi\ [exp(C_a\ X - C_a) - exp(-C_a)] + C_a^2\ \hat{\beta}\ (C_a + \hat{\beta})\}$$

Model 2 *(without the streamwise conduction term):*

$$N_{S2} = N_{HT2} + N_{FF2} = \underbrace{\left[\frac{\varpi\ \xi}{2\left(\varpi\ \bar{\theta}_2 + \frac{1}{C_k}\right)}\frac{\partial\bar{\theta}_2}{\partial X}\right]^2}_{N_{HT2}} + \underbrace{\frac{C_\mu \varpi\ Br'}{C_\mu \varpi\ \bar{\theta}_2 + 1}\left(\frac{\partial U}{\partial R}\right)^2}_{N_{FF2}}$$

$$= \underbrace{\frac{\{C_k\ \xi\ \hat{\beta}\ \varpi\ [C_b\ exp(-\hat{\beta}\ X) + C_c]\}^2}{4\{C_a\ \hat{\beta} - C_b\ C_k\ \varpi[exp(-\hat{\beta}\ X) - 1] + C_c\ C_k\ \hat{\beta}\ \varpi X\}^2}}_{N_{HT2}} + \underbrace{\frac{16\ C_a\ R^2\ \hat{\beta}\ \varpi\ Br'}{C_a\ \hat{\beta} - C_b\ C_k\ \varpi\ [exp(-\hat{\beta}\ X) - 1] + C_c\ C_k\ \hat{\beta}\ \varpi\ X}}_{N_{FF2}} \quad (16)$$

where: C_k - thermal conductivity ratio; C_μ - viscosity ratio; $\varpi = \frac{q_0^{''} D}{k_{eff}\ \bar{T}_0}$ - dimensionless heat flux; $\bar{T}_0$ – the mean temperature at the entrance, in K; $\xi = D/L$ - aspect ratio; $\hat{\beta} = \beta/L$ - dimensionless exponent of wall heat flux variation; β - exponent of wall heat flux variation, in m^{-1} ; $\bar{\theta}$ - dimensionless mean temperature; $Br' = \frac{\mu_f\ \bar{u}_f^2}{2\ r_0\ q_0''}$ - modified Brinkman number; X - Dimensionless longitudinal coordinate; $C_a = \frac{\gamma\ Pe}{C_\mu^{0.5}\ C_k\ \xi}$; $C_b = \frac{4}{C_k\ \xi^2}$; $C_c = 8\ Br' C_b$; $Pe = \frac{2\ r_0\ \bar{u}_f\ \rho_f\ c_{p,f}}{k_f}$ - the Peclet number.

The dimensionless temperature profiles, $\bar{\theta}_1$ and $\bar{\theta}_2$ are expressed as:

$$\bar{\theta}_1(X) = \{-C_a\, C_b\, [C_a\, exp(-\hat{\beta}\, X) - C_a + \hat{\beta}\, exp(C_a\, X - C_a - \hat{\beta}) - \hat{\beta}\, exp(-C_a - \hat{\beta})] + C_a\, C_c\, \hat{\beta}\, [C_a\, X + \hat{\beta}\, X - exp(C_a\, X - C_a) + exp(-C_a)] - C_c\, \hat{\beta}^2 [exp(C_a\, X - C_a) - exp(-C_a)]\}/[C_a^2\, \hat{\beta}\, (C_a + \hat{\beta})] \quad (17)$$

and

$$\bar{\theta}_2(X) = \frac{C_c\, \hat{\beta}\, X - C_b[exp(-\hat{\beta}\, X) - 1]}{C_a\, \hat{\beta}} \quad (18)$$

The results showed that the streamwise conduction affects the total entropy generation due to heat transfer irreversibility which is associated with the streamwise conduction, while the fluid friction irreversibility has an insignificant effect on the total entropy generation if the effect of streamwise conduction is considered (Fig. 5).

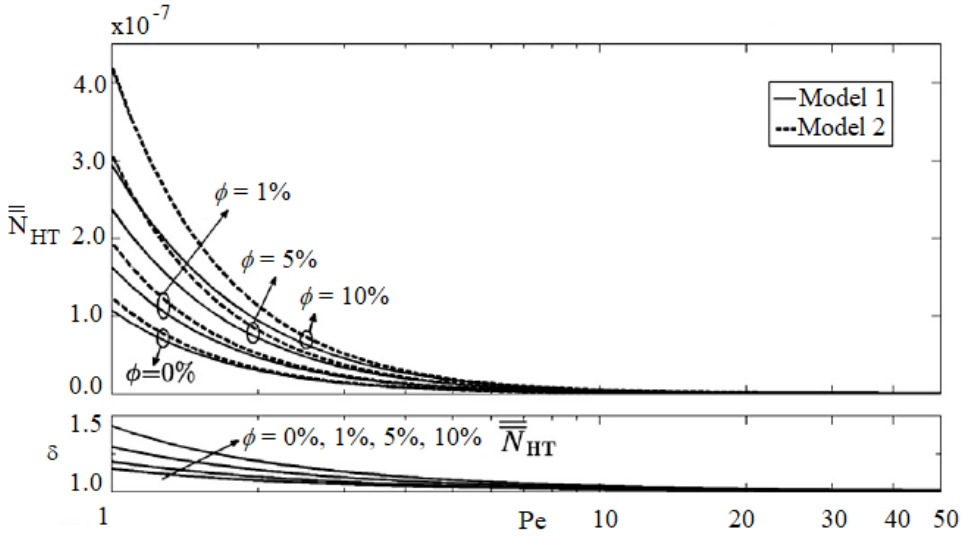

a)

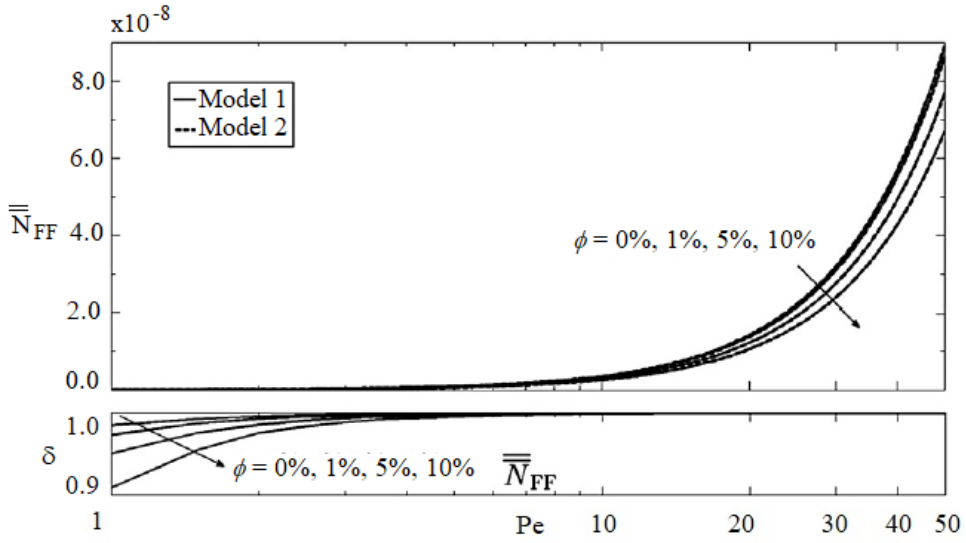

b)

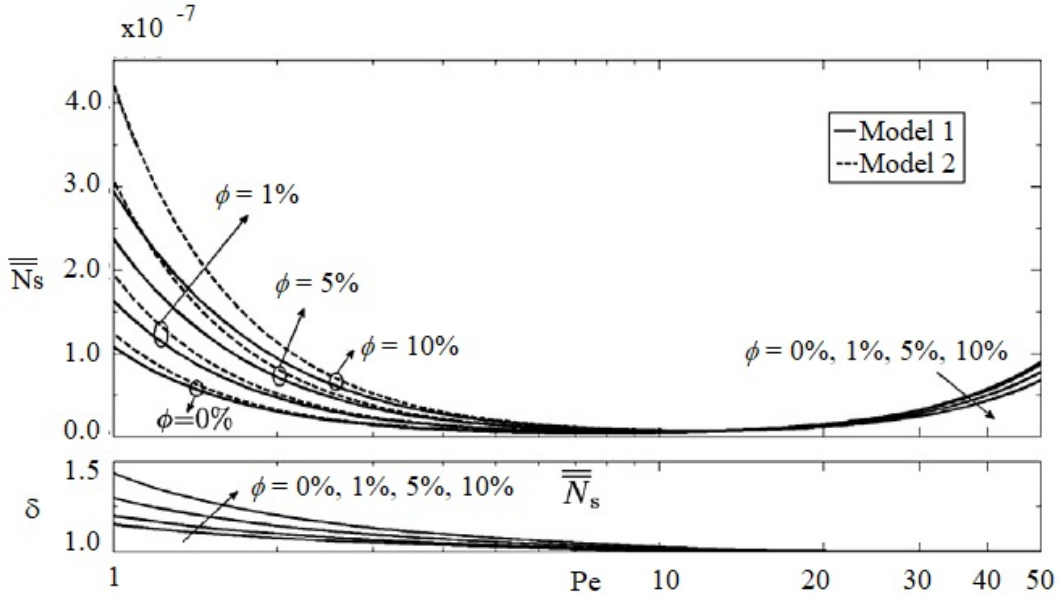

c)

Fig. 5. (a) The heat transfer irreversibility, (b) the fluid friction irreversibility, and (c) the total entropy generation for Model 1 and Model 2 and the corresponding ratio of discrepancy as a function of Peclet number with volume concentration of nanoparticles, ϕ [20]. Reprinted with permission from Elsevier.

They concluded, also, that if the fluid friction irreversibility is dominant (at higher Peclet number), the choice of working fluid becomes more important than the design of the microchannel.

2.1.4. Electromagnetic effect

It is known that the application of a magnetic field on the nanofluid flow leads to modifications to the flow structure and heat transfer, therefore on the entropy generation. Thus, the entropy generation in a 3D microchannel using Al_2O_3/water nanofluid under a magnetic field was numerical investigated by Hajialigol et al. [21]. In this study, in addition to the entropy generation due to heat transfer and fluid friction ireversibilities, the authors take into account the entropy generation due to the magnetic effects of the fluid. Thus, the local entropy generation equation becomes:

$$S''' = S_h''' + S_f''' + S_{MHD}''' = \underbrace{\left\{\frac{k_{nf}}{k_f}\frac{1}{(\theta+T^*)^2}\left[\left(\frac{\partial\theta}{\partial x}\right)^2+\left(\frac{\partial\theta}{\partial y}\right)^2+\left(\frac{\partial\theta}{\partial z}\right)^2\right]\right\}}_{S_h'''}$$
$$+\underbrace{\left\{\frac{1}{\theta+T^*}\frac{\mu_{nf}}{\mu_f}\,Ec\,Pr\left[2\left\{\left(\frac{\partial U}{\partial X}\right)^2+\left(\frac{\partial V}{\partial Y}\right)^2+\left(\frac{\partial W}{\partial Z}\right)^2\right\}+\left(\frac{\partial U}{\partial Y}+\frac{\partial V}{\partial X}\right)^2+\left(\frac{\partial V}{\partial Z}+\frac{\partial W}{\partial Y}\right)^2+\left(\frac{\partial W}{\partial X}+\frac{\partial U}{\partial Z}\right)^2\right]\right\}}_{S_f'''} \quad (19)$$
$$+\underbrace{\left\{\frac{1}{\theta+T^*}\frac{\sigma_{nf}}{\sigma_f}\,Ec\,Pr\,Ha^2\,(U^2+W^2)\right\}}_{S_{MHD}'''}$$

where T^*, Ec, Pr, Ha, U, V, W are defined as: $T^* = \frac{T\,k_f}{q''\,D_h}$, $Ec = \frac{k_f\,u_c^2}{q''\,(c_p)_f\,D_h}$ is the Eckert number, $Ha = B_0\,D_h\sqrt{\frac{\sigma_{nf}}{\rho_{nf}\,\upsilon_f}}$ is the Hartmann number, $U = \frac{u}{u_c}, V = \frac{v}{u_c}, W = \frac{w}{u_c}$ are the dimensionless velocity components , $\theta = \frac{T-T_c}{\Delta T}$ is the dimensionless temperature, u, v, w are electrical conductivity, X, Y, Z are the dimensionless Cartesian coordinates (=dimension/D_h);

Their analysis showed that total entropy generation decreases with increasing volume fraction and magnetic strength. The results indicated that the irreversibility due to the heat transfer has significant contribution to total entropy generation compared to flow friction irreversibility and the magnetic field (Fig. 6). Also it may be noted that the magnetic field effect is more significant than the flow friction irreversibility at the nanofluid flow through microchannel.

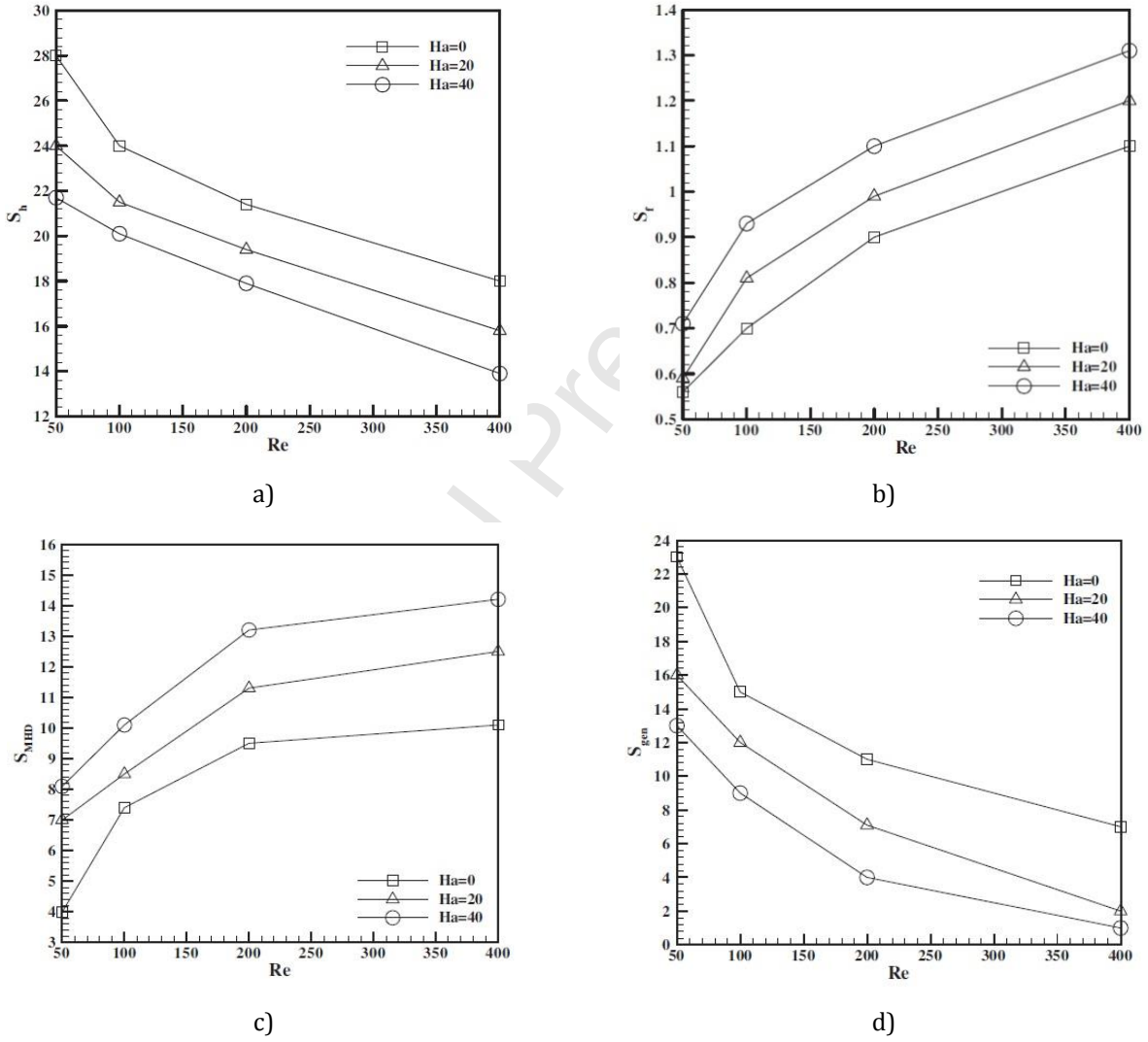

Fig. 6. Entropy generation versus Reynolds number for various Hartmann numbers: (a) thermal, (b) frictional, (c) magnetic and (d) total entropy generation (Aspect ratio = 0.1 and $\phi = 0.02$ [21]. Reprinted with permission from Elsevier.

Hosseini and Sheikholeslami [22] analytical studied the effect of MHD field on the entropy generation of the Al_2O_3/water nanofluid in a microchannel heat sink. In this paper, the dimensionless total entropy generation is given by:

$$N_s = \underbrace{N_{HT,s} + N_{HT,nf} + N_{HT,int}}_{N_{HT}} + N_{FF} + N_{MHD} \tag{20}$$

$$= \underbrace{\frac{\overline{\omega}^2}{(\overline{\omega}\,\theta_s + 1)^2}\left[\frac{L_{ch}^2}{L_x^2}\left(\frac{\partial \theta_s}{\partial x}\right)^2 + \left(\frac{\partial \theta_s}{\partial y}\right)^2\right]}_{N_{HT,s}}$$

$$+ \underbrace{\frac{k_{nf,eff}\,\overline{\omega}^2}{k_{s,eff}\,(\overline{\omega}\,\theta_s + 1)^2}\left[\frac{L_{ch}^2}{L_x^2}\left(\frac{\partial \theta_{nf}}{\partial x}\right)^2 + \left(\frac{\partial \theta_{nf}}{\partial y}\right)^2\right]}_{N_{HT,nf}}$$

$$+ \underbrace{D\,\overline{\omega}^2\left[\frac{\left(\theta_s - \theta_{nf}\right)^2}{(\overline{\omega}\,\theta_s + 1)(\overline{\omega}\,\theta_{nf} + 1)}\right]}_{N_{HT,int}} + \underbrace{\frac{\overline{\omega}\,Br'}{(\overline{\omega}\,\theta_{nf} + 1)}\left(\frac{d\widehat{U}}{dY}\right)^2}_{N_{FF}} + \underbrace{\frac{Ha^2\,\overline{\omega}\,Br'}{(\overline{\omega}\,\theta_{nf} + 1)}\,\widehat{U}^2}_{N_{MHD}}$$

where $D = \frac{h\,A_{pe}\,L_{ch}^2}{k_{s,eff}}$; $Br' = \frac{\mu_{nf}\,\overline{u}^2}{q_w\,L_{ch}}$ and $\overline{\omega} = \frac{q_w\,L_{ch}}{k_{s,eff}\,(T)_{w1.in}}$ is the dimensionless heat flux.

They concluded that N_s has its lowest value at the optimal Reynolds number of 2.35. After Re_{opt}, the N_s increases with increasing Reynolds number. The N_s decreases with an increase in Hartman number, from $Re_{opt} = 2.35$ to $Re_{opt} = 4.2$. When the Reynolds number passes Re_{cr}, N_s increases by increasing both Reynolds and Hartman numbers. It can be concluded that the application of the Lorentz forces is only useful for the Reynolds number up to Re_{cr} and then has a negative impact on thermal efficiency.

In another paper, the effects of magnetohydrodynamic (MHD) field and heat generation in the solid on entropy generation of the Al_2O_3/water nanofluid in a horizontal porous microchannel

heated symmetrically were analytical investigated by Hosseini et al. [23]. In this study, the viscous dissipation and heat generation were considered. The dimensionless entropy generation is defined as:

$$N_s = \underbrace{N_{HT,s} + N_{HT,nf} + N_{HT,int} + N_{HT,gen}}_{N_{HT}} + N_{FF} + N_{MHD} \tag{21}$$

$$= \underbrace{\frac{\overline{\omega}^2}{(\overline{\omega}\,\theta_s + 1)^2}\left[\xi^2\left(\frac{\partial\theta_s}{\partial x}\right)^2 + \left(\frac{\partial\theta_s}{\partial y}\right)^2\right]}_{N_{HT,s}}$$

$$+ \underbrace{\frac{k_{nf,eff}\,\overline{\omega}^2}{k_{s,eff}\,(\overline{\omega}\,\theta_s + 1)^2}\left[\xi^2\left(\frac{\partial\theta_{nf}}{\partial x}\right)^2 + \left(\frac{\partial\theta_{nf}}{\partial y}\right)^2\right]}_{N_{HT,nf}}$$

$$+ \underbrace{Bi\,\overline{\omega}^2\left[\frac{\left(\theta_s - \theta_{nf}\right)^2}{(\overline{\omega}\,\theta_s + 1)(\overline{\omega}\,\theta_{nf} + 1)}\right]}_{N_{HT,int}} + \underbrace{\frac{\Omega_{gen}\,\overline{\omega}}{\overline{\omega}\,\theta_s + 1}}_{N_{HT,gen}} + \underbrace{\frac{\overline{\omega}\,Br'}{(\overline{\omega}\,\theta_{nf} + 1)}\left(\frac{\widehat{U}^2}{Da} + \frac{d\widehat{U}}{dY}\right)^2}_{N_{FF}}$$

$$+ \underbrace{\frac{Ha^2\,\overline{\omega}\,Br'}{(\overline{\omega}\,\theta_{nf} + 1)}\,\widehat{U}^2}_{N_{MHD}}$$

where $\overline{\omega} = \frac{(q_{w1}+q_{w2})\,H}{2\,k_{s,eff}\,T_{w1,in}}$; $\xi = \frac{H}{L}$; $Bi = \frac{h_i\,a_i\,H^2}{k_s(1-\varepsilon)}$ - the Biot number; h_i - interstitial heat transfer coefficient ($Wm^{-2}\,K^{-1}$); H - microchannel half-height (m); k - effective thermal conductivity ratio; $Ha = B\,H\sqrt{\frac{\sigma_{nf}}{\mu}}$ - Hartman number; $B = Da\,Ha^2 + 1$; $Da = \frac{K}{L^2}$ - Darcy number; $Br' = \frac{2\,\mu_{eff}\,\overline{u}^2}{(q''_{w1}+q''_{w2})\,H}$ - modified Brinkman number; $\Omega_{gen} = \frac{2\,q'''_{gen}\,H}{q''_{w1}+q''_{w2}}$ - solid heat generation ratio.

The results concerning the impact of MHD without solid-phase heat generation showed that the value of minimum entropy generation decreases with the Hartman number rises, which shows the advantages to employ MHD field when the operating at the condition of $Re = Re_{op}$. When solid-phase heat generation is considered, it was noticed that the solid-phase heat generation irreversibility $N_{HT,gen}$ is higher than other irreversibilities, such that with the increase in

Reynolds number increases, N_s increases, and unlike the case of $\Omega_{gen} = 0$, no optimal value for Reynolds number was noticed (Fig. 7).

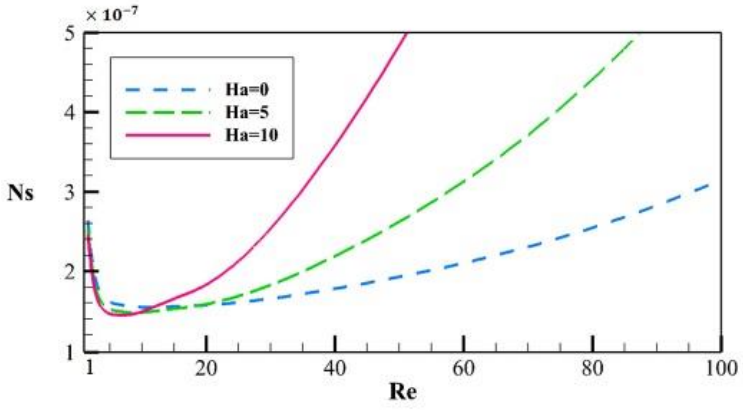

a)

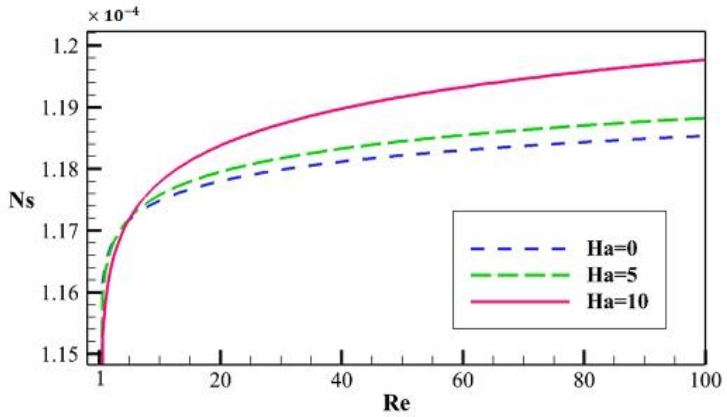

b)

Fig. 7. Total entropy generation a) the effect of MHD without solid-phase heat generation and b) the effect of solid-phase heat generation [23]. Reprinted with permission from Elsevier.

Ibáñez et al. [24] presented analytical studies on combined effects of hydrodynamic slip, magnetic field, suction/injection, thermal radiation, nanoparticle volume fraction and convective boundary conditions on the heat transfer and global entropy generation in Al_2O_3/water nanofluid flow through a microchannel with permeable plates. The local entropy generation rate, in

dimensionless terms, is defined by three terms: the first term is the irreversibility caused by heat flow in the nanofluid, the second term express the local the irreversibility due to fluid friction, while the third term represent the local entropy generation due to ohmic dissipation in the nanofluid, respectively. Thus:

$$\dot{S} = \underbrace{\frac{k_{nf}}{k_f}\frac{1}{\Theta^2}\left(\frac{\partial\Theta}{\partial y}\right)^2}_{N_{HT}} + \underbrace{\frac{Ec\ Pr}{\Theta}\frac{\eta_{nf}}{\eta_f}\left(\frac{du}{dy}\right)^2}_{N_{FF}} + \underbrace{\frac{Ec\ Pr}{\Theta}\frac{\sigma_{nf}}{\sigma_f}M^2\ u^2}_{N_{Ohm}} \tag{22}$$

where $\dot{S}$ is normalized by k_f/a^2. The global entropy generation rate, $<\dot{S}>$ is determined by integrating $\dot{S}$ in the whole volume occupied by the microchannel.

It was found that the minimum value of global entropy generation can be obtained at the optimum values of radiation parameter, nanoparticle volume fraction and Hartmann and Biot numbers. For example, the global entropy increases with the Hartmann number, M, and remains approximately constant with the radiation parameter, Rd (Fig. 8). The highest contribution in the global entropy generation is due to both heat conduction and viscous dissipation irreversibilities in the nanofluid, while the value of ohmic dissipation is lower.

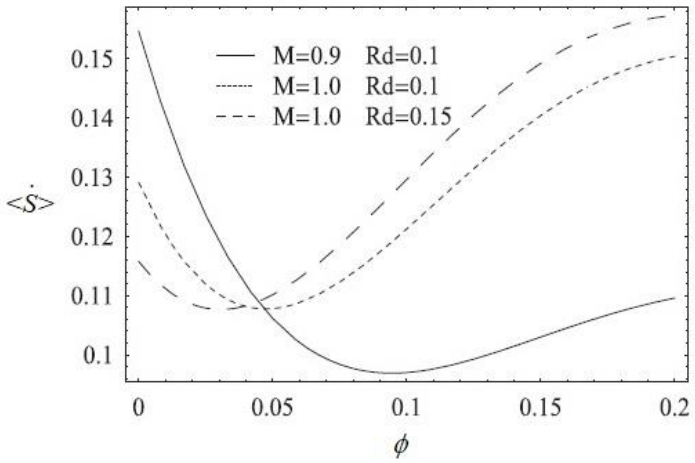

Fig. 8. Global entropy generation as a function of ϕ for different values of M and Rd. $Re = 3$; $\alpha = 0.01$; $P = 1$; $Ec = 1$; $Pr = 1, Bi = 0.8$ [24]. Reprinted with permission from Elsevier.

In another study, Lopez et al. [25] numerical investigated the effects of nonlinear thermal radiation, slip flow, nanoparticle volume fraction, suction/injection and convective-radiative boundary conditions on entropy generation in a MHD flow of Al_2O_3–water nanofluid through a porous vertical microchannel. The Runge–Kutta integration method with shooting technique was used for solved numerically of the dimensionless governing equations.

The local entropy generation, in dimensionless form is given by:

$$\dot{S} = \underbrace{\frac{(\theta_h - 1)^2}{[(\theta_h - 1)\theta + 1]^2}\left(\frac{k_{nf}}{k_f} + Rd[(\theta_h - 1)\theta + 1]^3\right)\left(\frac{\partial\theta}{\partial y}\right)^2}_{N_{HT}} + \underbrace{\frac{Br}{(\theta_h - 1)\theta + 1}\frac{\eta_{nf}}{\eta_f}\left(\frac{du}{dy}\right)^2}_{N_{FF}} + \underbrace{\frac{Br}{(\theta_h - 1)\theta + 1}Ha^2\frac{\sigma_{nf}}{\sigma_f}u^2}_{N_{Magnetic\ Field\ (MF)}} \tag{23}$$

where Ṡ is normalized by k_f/a^2.

In Eq. (23), the first term represent the heat transfer irreversibility, the last two terms represent irreverbilities due to fluid friction and magnetic field (Joule heating or Ohmic heating). The results reveled that the entropy generation decreases with decreasing both nanoparticle volume fraction and suction/ injection Reynolds number, while it increases with increasing Grashof number (Buoyancy force intensity), radiation parameter *Rd* and conduction-radiation parameter Nr.

Table 1 provides a summary of studies conducted on entropy generation in microchannel using nanofluid.

Table 1. Summary of works done on entropy generation in microchannel using nanofluid

Reference /Year	*Microchannel geometry*	*Nanofluid type and volume concentration*	*Flow regime*	*Remarks*
Theoretical studies				
Singh et al. [7]/2010		Al_2O_3/water $\phi \leq 5.0\%$	Laminar and turbulent	In laminar flow, the entropy generation rate ratio increases with the volume fraction; The use of the nanofluid is beneficial in turbulent flow (the entropy generation ratio decreases with the volume fraction).
Analytical studies				
Mah et al. [8]/2012	Circular	Al_2O_3/water $\phi \leq 8.0\%$	Laminar	If the viscous dissipation is considered, there is an increase of entropy generation with increasing volume fraction.
Sohel et al. [15]/2013	Circular	Al_2O_3/water Cu/water Al_2O_3/EG Cu/EG $\phi \leq 6.0\%$	Turbulent	For microchannel, the maximum decreasing rate in the entropy generation rate ratio was 36% using Cu/H2O nanofluid and 16% for Al2O3/H2O nanofluid, at a concentration of 6.0 %. For minichannel, the maximum reductions in the entropy generation rate ratio were 41% and 38% using Cu/H2O and Cu/EG nanofluid respectively, at the same nanoparticles concentration.
Ting et al. [20]/2014	Circular	Al_2O_3/water $\phi \leq 10.0\%$	Laminar	If the streamwise conduction is considered, total entropy generation decreases up to a threshold value with increasing Peclet number, after which there is an increase in total entropy generation with increasing Peclet number. Also, the effect of streamwise conduction on the total entropy generation is significant at low-Peclet-numbers and higher nanoparticle volume concentrations.
Ting et al. [19]/2015	Parallel plates	Al_2O_3/water $\phi \leq 4.0\%$	Laminar	In absence solid-phase heat generation, the entropy generation is minimum at $\Omega_w = 0.5$ and $Re_{opt} = 22$. If solid-phase heat generation is considered, the entropy generation is minimum at $\Omega_w = 0.75$, but in this case there is no an optimal Reynolds number. In this case, it can be notice that the entropy generation increases with the increase of Reynolds number.
Ibáñez et al. [24] /2016	Parallel plates	Al_2O_3/water $\phi \leq 0.2\%$	Laminar	The minimum values of global entropy, reached in optimum values of Hartmann, Biot, Eckert and suction/injection Reynolds number, decreased when

				nanoparticle volume fraction increased. The highest contribution in the global entropy generation is due to both heat conduction and viscous dissipation irreversibilities in the nanofluid, while the value of ohmic dissipation is lower.
Hosseini and Sheikholeslami [22]/2019	Rectangular	Al_2O_3/water $\phi \leq 4.0\%$	Laminar	By increasing of the Reynolds number to Re_{opt}, N_s decreases. Beyond Re_{opt}, the increase in Re enhance the S_{gen} and declines efficiency of the system. Applying the magnetic field is beneficial between $Re = 1.1$ and Re_{cr}, leading thus to minimum values of the entropy generation.
Hosseini et al. [23]/2019	Rectangular	Al_2O_3/water $\phi \leq 4.0\%$	Laminar	The value of minimum entropy generation decreases with the Hartman number rises, which shows the advantages to employ MHD field without solid-phase heat generation when the operating at the condition of $Re = Re_{op}$. When solid-phase heat generation is considered, N_s increases with increasing Reynolds number and unlike the case of $\Omega_{gen} = 0$, no optimal value for Reynolds number was noticed.
Numerical studies				
Mohammadian et al. [14] /2014		Al_2O_3/water $\phi \leq 4.0\%$	Laminar	Total entropy generation decreases with decreasing particles size and increasing volume fraction, the maximum performance being occurred at lower particles sizes and higher volume concentrations.
Yang et al. [13]/2015	Trapezoidal	$\phi \leq 4.0\%$	Laminar	They found that the highest thermal entropy generation was obtained near bottom and side walls because the difference between temperatures of the fluid and wall was significant, the effect thermal entropy being approximately three times higher than frictional effect.
Hajialigol et al. [21] /2015	Rectangular	Al_2O_3/water $\phi \leq 6.0\%$	Laminar	The heat transfer irreversibility has significant contribution to total entropy generation compared to fluid friction irreversibility and the magnetic field.
Ebrahimi et al. [10] /2016	Rectangular	Al_2O_3/water CuO/water $\phi \leq 3.0\%$	Laminar	The use nanofluids causes a reduction in entropy generation in microchannels with LVGs compared to pure water. The entropy generation rate due to the heat transfer irreversibility is much greater than that produced by the fluid friction irreversibility.
Maganti and	Rectangular	Al_2O_3/water	Laminar	For a given flow configuration, the magnitude of entropy

Dhar [11]/2017		$\phi \leq 5.0\%$		generation for nanofluids is higher compared to that of water, because the frictional resistance offered by the channel walls to a nanofluid is greater than that for water.
Lopez et al. [25]/2017	Parallel plates vertical	Al_2O_3/water $\phi \leq 0.2\%$	Laminar	The entropy generation decreases with decreasing both nanoparticle volume fraction and suction/ injection Reynolds number while it increases with increasing Grashof number (Buoyancy force intensity), radiation parameter *Rd* and conduction-radiation parameter Nr.
Heshmatian and Bahiraei [12]/2017	Circular	TiO_2/water $\phi \leq 4.0\%$	Laminar	The total entropy generation rate decreases with the increasing of the particle size due to the friction, which is the main cause of the entropy generation in the microchannel.
Alfaryjat et al. [17]/2019	Hexagon	Al_2O_3/water CuO/water SiO_2/water $\phi \leq 4.0\%$	Laminar	At low heat fluxes and high Reynolds numbers, water gives the lowest entropy generation, while at high heat flux the nanofluid has to be used in order to lower the overall irreversibility.
Al-Rashed et al. [18]/2019	Rectangular	CMC/CuO /water $\phi \leq 3.0\%$	Laminar	A reduction of 2.7% in the minimum total entropy generation rate of the nanofluid compared to the base fluid was reported.
Experimental studies				
Manay et al. [16]/2018	Rectangular	TiO_2/water $\phi \leq 20\%$	Laminar	The increase of height of the microchannel leads to the decrease in total entropy generation. By adding TiO_2 nanoparticles the thermal entropy generation decreases from 32.4% to 1.8% and the frictional entropy generation increases from 3.3% to 21.6%.

2.2. Entropy generation in minichannels

The effects of different shapes of boehmite alumina nanoparticles (platelets, blades, cylinders, and bricks) suspended in EG–water mixture and different tube materials (copper and steel) on the entropy generation in a minichannel based solar collector were analytical investigated by Mahian et al. [26] in laminar flow. The total entropy generation rate in the solar collector is calculated as:

$$\dot{S}_{gen} = \frac{\dot{W}_{lost}}{T_a} = \frac{\dot{E}_d + \dot{E}_l}{T_a} \tag{24}$$

$$= \underbrace{\eta_a\, G_t\, A_c \left(\frac{1}{T_p} - \frac{1}{T_s}\right) + \dot{m}\, c_p \left(\ln\left(\frac{T_{out}}{T_{in}}\right) - \frac{(T_{out} - T_{in})}{T_p}\right) + U_L\, A_c \left(1 - \frac{T_a}{T_p}\right)\left(\frac{T_p}{T_a} - 1\right)}_{\dot{S}_{gen,HT}}$$

$$+ \underbrace{\frac{\dot{m}\Delta P}{\rho_{nf}} \frac{\ln\left(\frac{T_{out}}{T_a}\right)}{(T_{out} - T_{in})}}_{\dot{S}_{gen,FF}}$$

where $\dot{m}$ is the total mass flow rate of nanofluid (kg/s), ΔP is the pressure drop (Pa), T_s is the apparent sun temperature (K), A_c is the surface area of solar collector (m^2), η_o is the optical efficiency of the glass cover, G_t is the solar radiation incoming on the glass cover (W/m^2), T_p is the plate temperature (K), T_a is the ambient temperature (K), and U_L is the overall heat loss coefficient (W/m^2K), $\dot{W}_{lost}$ is the amount of lost work (W), $\dot{E}_d$ is the destroyed exergy rate (W), $\dot{E}_l$ is the leakage exergy rate (W).

They concluded that for the copper tube the minimum entropy generation is obtained by using the nanofluid containing brick shaped particles with volume concentration of 2.0%, while for the steel tube, the minimum entropy generation is achieved by using blade shaped particles with volume concentration of 4.0%. The results also indicated that by using the copper tube instead of steel the total entropy generation rate could be reduced on average by 11% and 18% at a mass flow rate of 0.5 kg/s and 0.75 kg/s respectively.

In another paper, Mahian et al. [27] analytical studied the effects of using four different nanofluids (Cu/water, Al_2O_3/water, TiO_2/water, and SiO_2/water) on the performance of a minichannel flat plate solar collector in turbulent flow. For calculating the total entropy generation the equation (24) described in Ref. [26] is used. They found that by adding of

nanoparticles in the base fluid and high mass flow rates (i.e. 0.5 kg/s), the entropy generation is minimized. Also, the minimum and maximum values of entropy generation were noticed for Cu/water and SiO_2/water nanofluids.

Bahiraei and Abdi [28] developed a model for entropy generation of water-TiO_2 nanofluid flow in a circular minichannel considering the nanoparticle migration effect. Also, the effects of the Reynolds number, particle concentration and particle size on entropy generation are numerically investigated. The results obtained from the simulations were used for training of an Artificial Neural Network (ANN). The analysis were performed at Reynolds numbers of 500, 1000, 1500 and 2000, mean concentrations of 1.0, 2.0, 3.0 and 4.0%, particle sizes of 20, 40, 60 and 80 nm and for a constant wall heat flux of 10,000W/m^2.

Total entropy generation is defined as:

$$\dot{S} = \int \dot{S}''' \, dV = S'''_{HT} + S'''_{FF} \tag{25}$$

$$= \underbrace{\frac{k}{T^2}\left[\left(\frac{\partial T}{dx}\right)^2 + \left(\frac{\partial T}{dy}\right)^2\right]}_{S'''_{HT}} + \underbrace{\frac{\eta}{T}\left\{2\left[\left(\frac{\partial v_x}{dx}\right)^2 + \left(\frac{\partial v_y}{dy}\right)^2\right] + \left(\frac{\partial v_x}{dy} + \frac{\partial v_y}{dx}\right)^2\right\}}_{S'''_{FF}}$$

Their results indicated that the effect of particle migration on the entropy generation is significant for the large particles ($d_p = 80\ nm$) and high concentrations (4.0%), while this effect can be ignored for the fine particles ($d_p = 20\ nm$) and low concentration (1.0%).

The effects of the Reynolds number, particle size, wall heat flux, and particle concentration on entropy generation rates of water–Al_2O_3 nanofluid flow in a triangular minichannel was numerical investigated by Bahiraei and Majd [29]. The numerical simulations were performed for Reynolds numbers of 100, 300 and 500, wall heat fluxes of 1000, 2000 and 4000 W/m^2, concentrations of 1.0%, 2.0%, 3.0% and 5.0%, and nanoparticle sizes of 40, 60 and 80 nm. For the calculation of the local and global entropy generation, the Eq. (25) was used. They found that the total entropy generation decreases by increasing concentration, increasing Reynolds number, the decreasing heat flux and decreasing particle size. The total entropy generation rate has a minimum value for the particle size of 60 nm. Also, the total entropy generation rate is very low in large areas of the channel cross section at the higher Reynolds number due to the slower growth of the hydrodynamic and thermal boundary layers and, by default, lower values of the velocity and temperature gradients in larger areas from the central regions of the channel (Fig. 9).

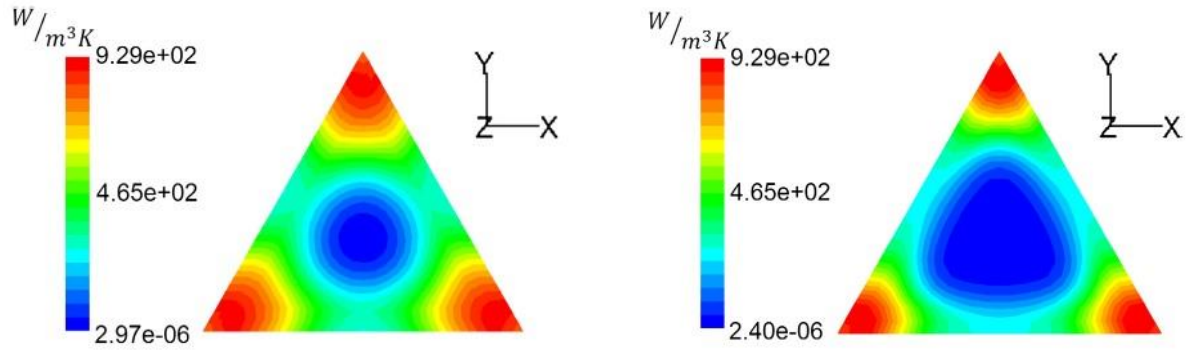

a) b)

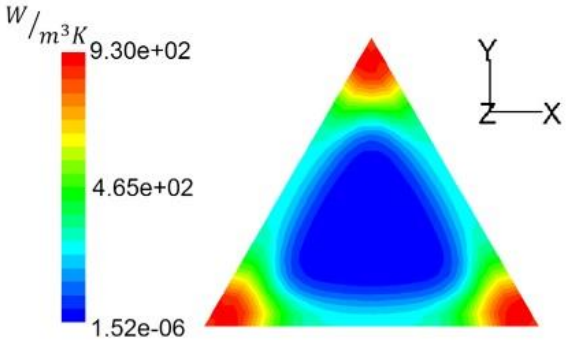

c)

Fig. 9. Contours of the total entropy generation rate at $q" = 4000\ W/m^2$, $d_p = 60\ nm$ and $\phi = 5\%$ through a cross section at 0.15 m distance from the inlet for: a) Re = 100, b) Re = 300, c) Re = 500 [29]. Reprinted with permission from Elsevier.

In another paper, Bahiraei et al. [30] numerical investigation the influence of volume concentration of nanoparticles (1.0, 3.0 and 4.0%), wall heat flux (40,000 W/m^2 and 60,000 W/m^2) and Reynolds number (100, 150 and 200) on entropy generation of non-Newtonian nanofluid flow within a C-shaped chaotic minichannel. The geometry and the dimensions of the channel are illustrated in Fig. 10.

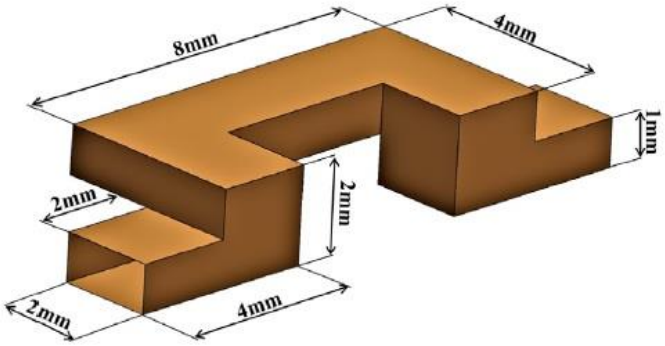

Fig. 10. C-shaped chaotic channel [30]. Reprinted with permission from Elsevier.

For the calculation of total entropy generation, the following relation was used:

$$\dot{S} = \int \dot{S}''' \, dV = S'''_{HT} + S'''_{FF} = \underbrace{\frac{k}{T^2}\left[\left(\frac{\partial T}{dx}\right)^2 + \left(\frac{\partial T}{dy}\right)^2 + \left(\frac{\partial T}{dz}\right)^2\right]}_{S'''_{HT}} + \underbrace{\frac{\eta}{T}\left\{2\left[\left(\frac{\partial v_x}{dx}\right)^2 + \left(\frac{\partial v_y}{dy}\right)^2 + \left(\frac{\partial v_z}{dz}\right)^2\right] + \left(\frac{\partial v_x}{dy} + \frac{\partial v_y}{dx}\right)^2 + \left(\frac{\partial v_x}{dz} + \frac{\partial v_z}{dx}\right)^2 + \left(\frac{\partial v_y}{dz} + \frac{\partial v_z}{dy}\right)^2\right\}}_{S'''_{FF}} \quad (26)$$

Their results showed that the total entropy generation decreases with increasing Reynolds number for concentrations of 0 and 3.0%. For the concentration of 4.0% the total entropy generation first decreases and then increases, the minimum value of entropy generation being at Re=150. This is because at low Reynolds numbers, the thermal entropy generation is more significant than the frictional entropy generation. Analyzing the results it can be concluded that, the total entropy generation in the chaotic channel is lower compared to the straight channel.

Later, Bahiraei et al. [31] numerical investigated the entropy generation of alumina–water, magnetite–water and copper-water flows in a chaotic minichannel. The geometrical dimensions of the channel are the same as those described in Ref. [30], namely the hydraulic diameter is $1.33\,mm$, the height and width of the rectangular cross section are $1\,mm$ and $2\,mm$, respectively. For the calculation of the local and global entropy generation, the Eq. (26) was used. The analyses were performed at the Reynolds numbers within the range 50-200, volume concentrations of 1.0, 2.0, 3.0 and 4.0% and for a wall heat flux of $10{,}000\ \mathrm{W/m^2}$. The results indicated that total entropy generation rate decreases by increasing the concentration for the copper–water and alumina–water nanofluids, while increases for the magnetite–water nanofluid (Fig. 11a). The minimum entropy generation rate was noticed for copper-water. The reason is that, the temperature gradient reduction with adding the nanoparticles is more significant for the Cu–water nanofluid. The results also revealed that total entropy generation rate reduces by

increasing Reynolds number for studied all nanofluids, the minimum and maximum entropy generation rates being related to the copper–water and magnetite–water nanofluids (Fig. 11b).

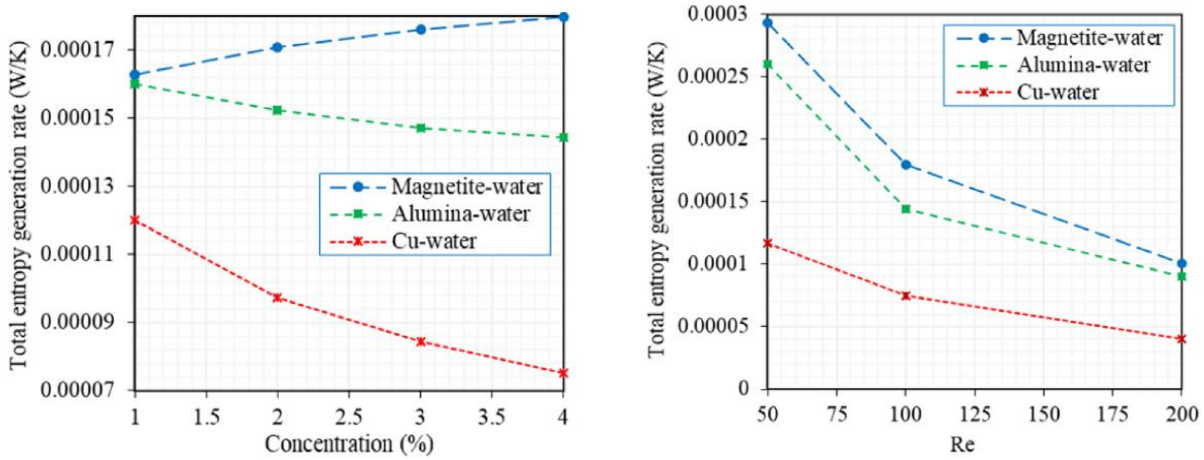

Fig. 11. Total entropy generation rate versus a) concentration and Re=100 and b) Reynolds number and $\phi = 4.0\%$ [31]. Reprinted with permission from Elsevier.

The effects of nanoparticle shape (cylindrical, brick, blade, platelet, and spherical) and Reynolds number on the entropy generation of boehmite alumina nanofluid ($\gamma - AlOOH$) flowing through a horizontal double-pipe minichannel heat exchanger were numerical analyzed by Al-Rashed et al. [32]. The minichannel heat exchanger consists of two concentric tubes with a length of 1 m, inner diameter of 1 mm, and outer diameter of 2 mm. Hot water and cold nanofluid flow through the annular region and inner tube, respectively. The simulations were carried out at Reynolds numbers within the range 500-200 for the tube side and at a constant Reynolds number for the annulus side *Re=1000,* at the inlet temperature of the nanofluid and water of 298 K and 308 K, and for nanoparticle concentrations of 0.5 to 2.0%. The results indicated that the nanofluid containing platelet shape and spherical shape nanoparticles have the highest and lowest rates of total entropy generation. They found also that total entropy generation rate increases with increasing Reynolds number.

Table 2 provides a summary of studies conducted on entropy generation in minichannel using nanofluid.

Table 2. Summary of works done on entropy generation in minichannel using nanofluid

Reference /Year	*Minichannel geometry*	*Nanofluid type and volume concentration*	*Flow regime*	*Remarks*
Analytical studies				
Mahian et al. [26]/2014	Flat plate	γ-AlOOH/EG-water $\phi \leq 4.0\%$	Laminar	By used the copper tube instead of the steel tube the total entropy generation rate could be reduced on average by 11% and 18% at a mass flow rate of 0.5 kg/s and 0.75 kg/s respectively. For the copper tube the minimum entropy generation is obtained by using the nanofluid containing brick shaped particles with volume concentration of 2.0%, while for the steel tube, the minimum entropy generation is achieved by using blade shaped particles with volume concentration of 4.0%.
Numerical studies				
Mahian et al. [27]/2014	Flat plate	Cu/water Al_2O_3/water TiO_2/water SiO_2/water $\phi \leq 4.0\%$	Turbulent	The minimum and maximum values of entropy generation were noticed for Cu/water and SiO_2/water nanofluids.
Bahiraei and Abdi [28] /2016	Circular	TiO_2/water $\phi \leq 4.0\%$	Laminar	The effect of particle migration on the entropy generation is become significant at the large particles ($d_p = 80$ nm) and high concentrations (4.0%), while this effect can be ignored for the fine particles ($d_p = 20$ nm) and low concentration (1.0%).
Bahiraei and Majd [29] /2016	Triangular	Al_2O_3/water $\phi \leq 5.0\%$	Laminar	Total entropy generation decreases by increasing concentration, increasing Reynolds number, the decreasing heat flux and decreasing particle size.
Bahiraei et al. [30]/2017	C-shaped	CMC-TiO_2 /water $\phi \leq 4.0\%$	Laminar	Total entropy generation decreases with increasing Reynolds number for concentrations of 0 and 3%. For the concentration of 4.0% the total entropy generation first decreases and then increases, the minimum value of entropy generation being at Re=150.
Bahiraei et al.	C-shaped	Al_2O_3/water	Laminar	Total entropy generation rate reduces by increasing

[31]/2018		Fe_3O_4/water Cu/water $\phi \leq 4.0\%$		Reynolds number for studied all nanofluids, the minimum and maximum entropy generation rates being related to the copper–water and magnetite–water nanofluids.
Al-Rashed et al. [32]/2019	Circular	γ-AlOOH/EG-water $\phi \leq 2.0\%$	Laminar	The boehmite alumina nanofluid containing platelet shape and spherical shape nanoparticles have the highest and lowest rates of total entropy generation. Also, total entropy generation rate increases with increasing Reynolds number.

2.3. Entropy generation in cavities

Natural and mixed convection heat transfer as well as the entropy generation of nanofluids in cavities are important topics in thermal applications (i.e. cooling and heating systems, solar collectors, nuclear reactors, storage tanks) [33-39].

2.3.1 Porous cavities

In last years, the studies on the entropy generation of nanofluids in porous cavities have attracted considerable attention [40-49]. For example, Kefayati [40] analyzed the entropy generation rate in a porous square cavity filled with a non-Newtonian nanofluid (Cu-water). Finite Difference Lattice Boltzmann Method (FDLBM) is used. Analyses have been performed in laminar natural convection for the following parameters: the Rayleigh number, $Ra = 10^4$ and $Ra = 10^5$, the power-law index, $n = 0.6 - 1.0$, Darcy number, $Da = 10^{-3} - 10^{-1}$ and the volume fractions of nanoparticles, $\phi = 0.02$ and $\phi = 0.04$.

The dimensionless entropy generation is given by following equation:

$$\dot{S}_S = \dot{S}_T + \dot{S}_F = \overline{\dot{S}}_S \times \frac{T_0^2\, L^2}{k_{nf}\Delta T^2} = \left(\overline{\dot{S}}_T + \overline{\dot{S}}_F\right) \times \frac{T_0^2\, L^2}{k_{nf}\Delta T^2} \tag{27}$$

$$= \left\{ \underbrace{\frac{k_{nf}}{T_0^2}\left[\left(\frac{\partial \overline{T}}{\partial \overline{x}}\right)^2 + \left(\frac{\partial \overline{T}}{\partial \overline{y}}\right)^2\right]}_{\overline{\dot{S}}_T} + \underbrace{\frac{\overline{\mu}_{nf}}{T_0\, K}\left[\overline{u}^2 + \overline{v}^2\right] + \frac{\overline{\mu}_{nf}}{T_0}\left[2\left(\frac{\partial \overline{u}}{\partial \overline{x}}\right)^2 + 2\left(\frac{\partial \overline{v}}{\partial \overline{y}}\right)^2 + \left(\frac{\partial \overline{u}}{\partial \overline{y}} + \frac{\partial \overline{v}}{\partial \overline{x}}\right)^2\right]}_{\overline{\dot{S}}_F} \right\}$$

$$\times \frac{T_0^2\, L^2}{k_{nf}\Delta T^2}$$

$$= \underbrace{\frac{k_{nf}}{k_f}\left[\left(\frac{\partial T}{\partial x}\right)^2 + \left(\frac{\partial T}{\partial y}\right)^2\right]}_{\dot{S}_T} + \underbrace{\Phi_l\left[u^2 + v^2 + Da\left[2\left(\frac{\partial u}{\partial x}\right)^2 + 2\left(\frac{\partial v}{\partial y}\right)^2 + \left(\frac{\partial u}{\partial y} + \frac{\partial v}{\partial x}\right)^2\right]\right]}_{\dot{S}_F}$$

where

$$\Phi_l = \frac{\mu_{nf}\, T_0}{k_f}\left(\frac{\alpha_f}{L\,\Delta T}\right)^2 Ra = \frac{\left\{2\left[\left(\frac{\partial u}{\partial x}\right)^2 + \left(\frac{\partial v}{\partial y}\right)^2\right] + \left(\frac{\partial u}{\partial y} + \frac{\partial v}{\partial x}\right)^2\right\}^{\frac{(n-1)}{2}} T_0}{(1-\phi)^{2.5}\, k_f}\left(\frac{\alpha_f}{L\,\Delta T}\right)^2 Ra \tag{28}$$

Their results showed that the increase of nanofluid volume fraction leads to increasing entropy generation at different Rayleigh numbers, power-law indexes, and Darcy numbers. In another study, Kefayati [41] investigated natural convection of non-Newtonian shear-thinning nanofluid in a porous cavity using the same method, Finite Difference Lattice Boltzmann. The study has been carried out in following conditions: Rayleigh number ($Ra = 10^4$ and 10^5), Darcy number ($Da = 0 - 0.01$), Prandtl number ($Pr = 0.1 - 10.0$), Buoyancy ratio number ($N_r = 0.1 - 4.0$), power-law index ($n = 0.4 - 1.0$), Lewis number ($Le = 1 - 10$), Thermophoresis parameter ($N_t = 0.1 - 1.0$), and Brownian motion parameter ($N_b = 0.1 - 5.0$). In this study, the local dimensionless entropy generation is defined as the sum of the irreversibilities due to thermal gradients, viscous dissipation and concentration gradients:

$$\dot{S}_S = \dot{S}_T + \dot{S}_F + \dot{S}_D \tag{29}$$
$$= \underbrace{\left[\left(\frac{\partial T}{\partial x}\right)^2 + \left(\frac{\partial T}{\partial y}\right)^2\right]}_{\dot{S}_T} + \underbrace{\Phi_I\left[u^2 + v^2 + Da\left[2\left(\frac{\partial u}{\partial x}\right)^2 + 2\left(\frac{\partial v}{\partial y}\right)^2 + \left(\frac{\partial u}{\partial y} + \frac{\partial v}{\partial x}\right)^2\right]\right]}_{\dot{S}_F}$$
$$+ \underbrace{\Phi_{II}\left[\left(\frac{\partial C}{\partial x}\right)^2 + \left(\frac{\partial C}{\partial y}\right)^2\right] + \Phi_{III}\left[\left(\frac{\partial C}{\partial x}\right)\left(\frac{\partial T}{\partial x}\right) + \left(\frac{\partial C}{\partial y}\right)\left(\frac{\partial T}{\partial y}\right)\right]}_{\dot{S}_D}$$

where the variables Φ_I, Φ_{II} and Φ_{III} are defined as:

$$\Phi_I = \frac{\mu\, T_0}{k}\left(\frac{\alpha}{L\,\Delta T}\right)^2 Ra = \frac{\left\{2\left[\left(\frac{\partial u}{\partial x}\right)^2 + \left(\frac{\partial v}{\partial y}\right)^2\right] + \left(\frac{\partial u}{\partial y} + \frac{\partial v}{\partial x}\right)^2\right\}^{\frac{(n-1)}{2}} T_0}{k}\left(\frac{\alpha}{L\,\Delta T}\right)^2 Ra \tag{30}$$
$$= \left\{2\left[\left(\frac{\partial u}{\partial x}\right)^2 + \left(\frac{\partial v}{\partial y}\right)^2\right] + \left(\frac{\partial u}{\partial y} + \frac{\partial v}{\partial x}\right)^2\right\}^{\frac{(n-1)}{2}} \lambda$$

$$\Phi_{II} = \frac{R\,D\,T_0}{k\,C_0}\left(\frac{\Delta C}{\Delta T}\right)^2 \tag{31}$$

$$\Phi_{III} = \frac{R\,D}{k}\left(\frac{\Delta C}{\Delta T}\right) \tag{32}$$

and have values $\Phi_{II} = 0.5$, $\Phi_{III} = 0.01$ and $\lambda = 0.01$.

They found that the entropy generation due to fluid friction was significantly affected against power-law index compared to the entropy generation due to heat and mass transfer. Also, the increase in Darcy, Lewis, Buoyancy ratio numbers leads to increasing total entropy generation, while the total entropy generation has a different trend (initially decreases up to $N_t = N_b = 0.5$, after which it increases) with increasing the Brownian motion and Thermophoresis parameters.

A similar study was also performed by Hoseinpour et al. [42] which studied the entropy generation of a nanofluid in a porous cavity using Lattice Boltzmann Method. In this study, they concluded that it could be possible to minimize the entropy generation in the system if the porosity of the medium is varied and also, that the entropy generation is a decreasing function of the nanofluid volume fractions.

Siavashi et al. [43] numerical analyses the effects of the number of fins and their length on entropy generation of Cu-water nanofluid inside a cavity with porous fins located on heated wall using two models, one for the nanofluid (two-phase model) and other for the porous region (Darcy–Brinkman–Forchheimer model). The porous fins have constant thickness of $0.04 \cdot H$, thermal conductivity of $k_s = 10 \cdot k_{bf}$ and porosity of 0.9. The study was carried out for various fins' lengths defined as ratios between the fin length (L_f) and cavity length (H) of $L_f/H = 0.3, 0.6$ and 0.9 and different numbers of fins, $N_f = 0, 1.0, 2.0$ and 3.0. Various nanoparticles fractions, $\phi = 0.01, 0.02, 0.03$ and 0.04, Rayleigh numbers ($Ra = 10^4 - 10^6$) and Darcy numbers ($Da = 10^{-1} - 10^{-4}$) were investigated. The results indicated that the use porous fins diminished the entropy generation, the increase of the number of fins leading to decreasing entropy generation (Fig. 12).

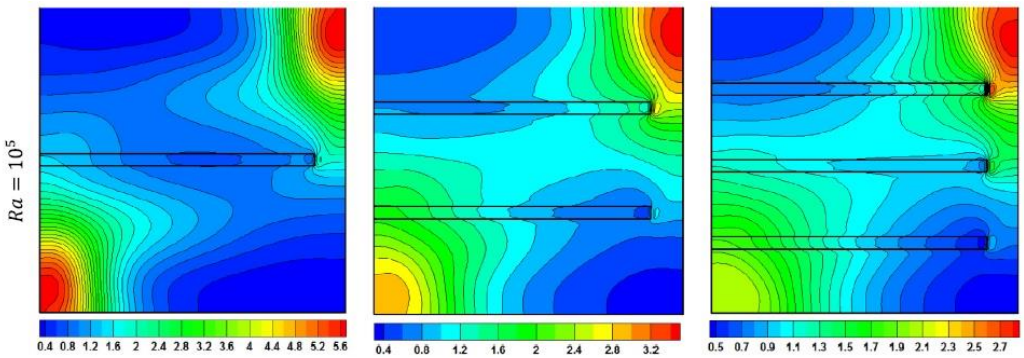

Fig. 12. Distribution of total entropy generation for different N_f [43]. Reprinted with permission from Elsevier.

Later, Goqo et al. [44] studied the entropy generation in a square cavity filled with porous medium saturated by nanofluid using the multivariate spectral quasilinearisation method. The schematic of the problem is shown in Fig. 13. A magnetic field is applied in the $\overline{x}$ direction. For modeling the flow in the porous media, the Darcy-Boussinesq model was employed. Their findings disclosed that an increase in Rayleigh number leads to the increase entropy generation when there is particle Brownian motion and that the total entropy generation reduces as the radiation parameter increases for various Hartman number values.

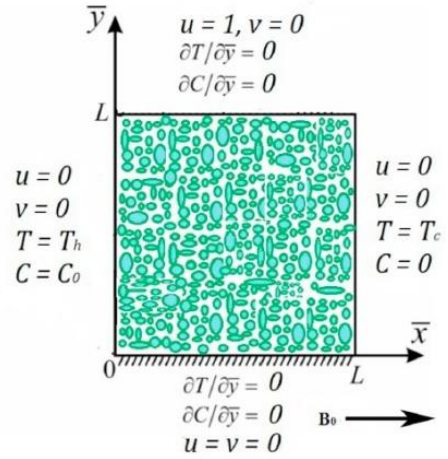

Fig. 13. Schematic of the problem considered by Goqo et al. [44]. Reprinted with permission from Elsevier.

In another work, Baghsaz et al. [45] studied the effect of nanoparticle sedimentation on entropy generation in a completely porous cavity filled with Al_2O_3/water nanofluid. In this study, some assumptions were performed: the nanofluid has Newtonian fluid behavior, the porous medium was considered to be homogeneous and isotropic and also the thermo-physical properties of the porous medium were considered identical to those of the base fluid.

The non-dimensional form of entropy generation rate was defined as follows:

$$\dot{S}_{gen} = \dot{S}_{HT} + \dot{S}_{FF} \tag{33}$$
$$= \frac{\mu_{nf}\,\alpha_{bf}^2}{T_0}\left[\left(\frac{\partial\theta}{\partial X}\right)^2 + \left(\frac{\partial\theta}{\partial Y}\right)^2\right] + \frac{T_0\,\mu_{nf}\,\alpha_{bf}^2\,L^2}{k_{bf}\,K\,(T_h - T_c)^2}\,(u_m^{*2} + v_m^{*2})$$
$$+ \frac{T_0\,\mu_{nf}\,\alpha_{bf}^2}{k_{bf}\,(T_h - T_c)^2}\left[2\left(\frac{\partial u_m^*}{\partial X}\right)^2 + 2\left(\frac{\partial v_m^*}{\partial Y}\right)^2 + \left(\frac{\partial u_m^*}{\partial Y} + \frac{\partial v_m^*}{\partial X}\right)^2\right]$$

where the first term represents the entropy generation due to the heat transfer, and the second and third terms are entropy generations due to the Darcy and viscous dissipations, respectively.They revealed that, remarkably high entropy generation rates were noticed near cold and hot walls, due to the high temperature and velocity gradients in these regions and also that with increasing the Ra number, the entropy generation rate increases.

The analysis of entropy generation in magnetohydrodynamic nanofluid flow inside an enclosure filled with a fluid saturated porous medium is made by Malik and Nayak [46] numerically. The flow is influenced by time periodic discrete heat sources along the short side walls. Schematic of the cavity is shown in Fig. 14. The analyses were performed for following conditions: Grashof number (10^4— 10^6), Hartmann number (1– 50), Darcy number (0.001– 1.0) and nanoparticle volume fraction (0.0–0.20) with a fixed Prandtl number (6.2). Their results can be summarized as: i) the high values of Grashof number lead to increased entropy generated; ii) the heat transfer irreversibility is dominant compared to magnetic field and fluid friction irreversibility; iii) the total entropy generation increases with increasing volume fraction for all studied Da numbers; iv) the optimum value for minimum entropy generation is obtained at $Da = 0.001$ and $\phi = 0.2$ for $Gr = 10^6$ and $Ha = 50$.

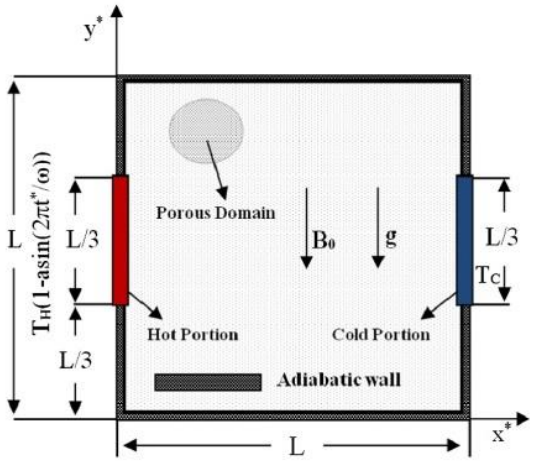

Fig. 14. Physical configuration of the problem considered by Malik and Nayak [46]. Reprinted with permission from Elsevier.

In another study, Ghasemi and Siavashi [47] studied the effects of nanofluid fraction ($\phi = 0.02 - 0.12$), Rayleigh number ($Ra = 10^3 — 10^6$), Hartmann number ($Ha = 0 – 20$) and porous-fluid thermal conductivity ratio ($K^* = 1 – 70$) on entropy generation in a square porous enclosure using a parallel Lattice Boltzmann code. In this study, the total entropy generation is computed as the sum between the entropy generation due to fluid flow friction and viscous dissipation (frictional), the infinitesimal temperature gradient (thermal) and the magnetic field effects (magnetic). They found that the minimum and the maximum total entropy generation were noticed at $Ha = 10$ and $Ha = 15$ respectively. Also, the thermal and frictional entropy generation terms were dominant for $Ra = 10^3$ and $Ra = 10^5$, respectively, while for $Ra = 10^4$ all the frictional, thermal and magnetic irreversibility terms have the same order of magnitude.

Fersadou et al. [48] studied the effect of magnetic field on entropy generation within a vertical porous channel filled with Cu-water nanofluid. The volume control method was used to solve equations. The total entropy generation was calculated as sum between the total entropy generations due to temperature gradients, $\dot{S}_{T\square}$, friction, $\dot{S}_{Fr}$, and hydromagnetic effect, $\dot{S}_{Mag}$:

$$\dot{S}_{gen} = \dot{S}_{Th} + \dot{S}_{Fr} + \dot{S}_{Mag} \tag{34}$$
$$= \underbrace{\int R_k \frac{k_{nf}}{k_f}\left\{\left(\frac{\partial\theta}{\partial X}\right)^2 + \left(\frac{\partial\theta}{\partial Y}\right)^2\right\} dv}_{\dot{S}_{Th}}$$
$$+ \underbrace{\int \left[\varphi\, \varepsilon\, R_\mu \frac{\mu_{nf}}{\mu_f}\, \Phi + \frac{\varphi\, \varepsilon^2}{Da}\frac{\mu_{nf}}{\mu_f}(U^2+V^2)\right] dv}_{\dot{S}_{Fr}} + \underbrace{\int \varphi\, \varepsilon^2\, Ha^2 \frac{\sigma_{nf}}{\sigma_f}\, U^2\, dv}_{\dot{S}_{Mag}}$$

where $\Phi = 2\left(\frac{\partial u}{\partial x}\right)^2 + 2\left(\frac{\partial v}{\partial y}\right)^2 + \left(\frac{\partial u}{\partial y} + \frac{\partial v}{\partial x}\right)^2$ is the viscous dissipation function, $\varphi = \mu_f\, U_i^2\, T_0 k_f / q^2\, H^2$ is the irreversibility coefficient.

Results showed that at small Hartmann numbers the entropy generation increases due to increase in the friction and also that, adding of nanoparticles in the base fluid increases the total entropy generation due to friction and hydromagnetic effect, while the thermal irreversibility has almost no variation with volume friction.

The influence of the internal heat generation/ absorption and chemical reaction on the double diffusive mixed convective nanofluid nanofluid flow and entropy generation in a square porous lid driven cavity was carried out by Hussain et al. [49]. A monolithic Galerkin finite element approach together with geometric multigrid technique has been adopted to solve governing equations. The dimensionless forms of the local entropy generation in this work were defined as follows:

$$\dot{S}_{gen,l} = \dot{S}_{HT,l} + \dot{S}_{FF,l} + \dot{S}_{DC,l} = \underbrace{\frac{k_{nf}}{k_f}\left[\left(\frac{\partial\theta}{\partial X}\right)^2 + \left(\frac{\partial\theta}{\partial Y}\right)^2\right]}_{\dot{S}_{HT,l}} + \tag{35}$$
$$\underbrace{\frac{\varphi_1}{Da}(U^2+V^2) + \varphi_1 \frac{\mu_{nf}}{\mu_f}\left[2\left(\frac{\partial U}{\partial X}\right)^2 + 2\left(\frac{\partial V}{\partial Y}\right)^2 + \left(\frac{\partial U}{\partial Y} + \frac{\partial V}{\partial X}\right)^2\right]}_{\dot{S}_{FF,l}} +$$

$$\underbrace{\varphi_2\left[\left(\frac{\partial C}{\partial X}\right)^2+\left(\frac{\partial C}{\partial Y}\right)^2\right]+\varphi_3\left[\left(\frac{\partial C}{\partial X}\right)\left(\frac{\partial \theta}{\partial X}\right)+\left(\frac{\partial C}{\partial Y}\right)\left(\frac{\partial \theta}{\partial Y}\right)\right]}_{\dot{S}_{DC,l}}$$

where φ_1, φ_2 and φ_3 are the irreversibility ratios and were expressed as:

$$\varphi_1 = \frac{\mu\, T_0}{k}\left(\frac{U_0}{T_h - T_c}\right)^2 \tag{36}$$

$$\varphi_2 = \frac{R\, D_e}{c_o}\,\frac{T_0}{k}\left(\frac{c_h - c_c}{T_h - T_c}\right)^2 \tag{37}$$

$$\varphi_3 = \frac{R\, D_e}{c_o}\left(\frac{c_h - c_c}{T_h - T_c}\right)^2 \tag{38}$$

They noticed an increase in average entropy generation due to heat transfer irreversibility with the enhancement in Richardson number, nanoparticles volume fraction, Darcy number and porosity parameter, whereas a decrease has been noticed in it with an increase in heat generation/absorption parameter, chemical reaction parameter and Lewis number. Also, the average entropy generation due to fluid friction rises with an amplification in heat generation/absorption parameter, Richardson number and nanoparticles volume fraction, while it reduces with an increase in the chemical reaction parameter, Darcy number, porosity parameter and Lewis number. An increase is observed in dimensionless entropy generation due to solutal concentration with an enhancement in Richardson number, Darcy number and porosity parameter, whereas a decrease has been noticed in it with an increase in heat generation/absorption parameter; chemical reaction parameter and Lewis number. Finally, the entropy generations due to the heat transfer and fluid friction increases with an augmentation in volume fraction, whereas entropy generation due to solutal concentration decreases with an enhancement in volume fraction.

2.3.2. The magnetic field effect on entropy generation

The effect of the external oriented magnetic field on entropy generation of Cu–water nanofluid flow in an open cavity in laminar flow was numerical studied by Mehrez et al. [50]. The analyses were performed for the Hartmann, Reynolds and Richardson numbers in the range 0-200, 100-500 and 0.001-1 respectively. The volume fractions were within the range 0.02-0.06 and inclination angles of the magnetic field considered in this paper were 0°, 45° and 90° respectively. The aspect ratio of the computational domain defined as the ratio between the length and the height of the channel was fixed at $l/w = 3.5$ and the aspect ratio of the cavity defined as the ratio between the length and the height of the cavity was $\mathrm{L/H} = 2$.

The nondimensional entropy generation is defined as:

$$\dot{S}_{gen} = \underbrace{\frac{k_{nf}}{k_f}\left[\left(\frac{\partial\theta}{\partial X}\right)^2 + \left(\frac{\partial\theta}{\partial Y}\right)^2\right]}_{\dot{S}_{gen,C}} + \underbrace{\chi\,\frac{\mu_{nf}}{\mu_f}\left[2\left(\frac{\partial U}{\partial X}\right)^2 + 2\left(\frac{\partial V}{\partial Y}\right)^2 + \left(\frac{\partial U}{\partial Y} + \frac{\partial V}{\partial X}\right)^2\right]}_{\dot{S}_{gen,V}} + \underbrace{\chi\, Ha^2\,\frac{\sigma_{nf}}{\sigma_f}\,(U\sin\gamma - V\cos\gamma)^2}_{\dot{S}_{gen,M}} \tag{39}$$

where $\dot{S}_{gen,C}$, $\dot{S}_{gen,V}$, $\dot{S}_{gen,M}$ - the dimensionless entropy generation due to conduction, viscous effects and magnetic field, respectively, $\chi = \frac{\mu_f T_0}{k_f}\left(\frac{u_0}{T_H - T_C}\right)^2$ is the irreversibility factor.

They found that at $\gamma = 0°$ (horizontal magnetic field), the entropy generation decreases by increasing both the Hartmann number (due to the attenuation of the flow intensity) and volume fraction. Applying the magnetic field, the entropy generation could be reduced if the Reynolds and/or Richardson numbers increase. At $\gamma = 45°$ and $\gamma = 90°$ the entropy generation significantly increases by the intensification of the magnetic field and the increasing both the Hartmann number and volume fraction.

The entropy generation analysis in a trapezoidal enclosure filled with Cu-water nanofluid considering the effect of magnetic field was performed by Aghaei et al. [51]. The study was conducted for following parameters: $Gr = 10^4$, $Re = 30 - 1000$, $Ha = 25 - 100, \varphi = 0.01 - 0.04$ and side-wall angle with the horizon $\theta_s = 15° - 60°$. The finite volume method and SIMPLER algorithm have been utilized to solve the governing equations. It is shown that for all Reynolds numbers and volume fractions with augmentation Hartmann number, the total entropy generation decreases. Also, by increasing Hartmann number, the total entropy generation up to reach more θ_s, has decreasing behavior and then has increasing trend.

The entropy generation in a partially heated two sided lid driven cavity under magnetic field effect using Al_2O_3-water nanofluid was numerical investigated by Hussain et al. [52]. Two heat sources on the lower wall of the cavity were fixed and the remaining part of the bottom wall was kept insulated. Top wall and vertically moving walls were also maintained at constant cold temperature. Galerkin weighted residual finite element method has been adopted to solve governing equations. They concluded that with the entropy generations due to heat transfer, fluid friction and also magnetic field, as well as the total entropy generation increases with an increase in Reynolds number and volume fraction. This increase in entropy generation is mostly due to heat transfer. Fluid friction and magnetic field play a little role in increase of entropy generation.

Mahmoudi et al. [33] analyzed the nanofluid flow in a cavity along with heat generation/absorption and entropy effects and they found that heat generation/absorption parameter has no effect on entropy for $-10 < q < 5$. The results indicated also that addition of nanoparticles leads to reduction of the entropy generation. Sheikholeslami and Ganji [53]

numerically investigated the magnetohydrodynamic free convection flow of CuO–water nanofluid in a square enclosure with a rectangular heated body using Lattice Boltzmann Method (LBM) scheme. The authors found that the dimensionless entropy generation number increase with increasing Rayleigh number and nanoparticle volume fraction, but it decreases with increasing Hartmann number.

The influence of a magnetic field on the entropy generation of Cu–water nanofluid in a cavity with complex-wavy surfaces was studied by Cho [54]. In this study, the effects of the Hartmann number, Rayleigh number, Eckert number, nanoparticle volume fraction, and wavy-wall geometry parameters on the entropy generation were examined. The some findings of the analysis can be summarized as follows:

- the magnetic field effect has a insignificant effect on the velocity and temperature field for a given low Rayleigh number, and thus, the total entropy generation have a lesser variation with increasing Hartmann number;
- given a high Rayleigh number, the total entropy generation increases with increasing Hartmann number;
- a minimal total entropy generation can be noticed at a given appropriate wavelength of the wavy surface;
- the total entropy generation increases with increasing wave amplitude of the wavy surface.

In another work, Cho [55] numerically studied the effects of an inclined magnetic field on the mixed convection heat transfer performance and entropy generation rate in a wavy-wall lid-

driven cavity filled with Cu-water nanofluid. An inclination angle of magnetic field of $\gamma = 90°$ and $\gamma = 270°$ respectively, result in a larger total entropy generation, while inclination angles of $\gamma = 0°$ and $\gamma = 180°$, lead to a smaller total entropy generation, in the natural convection-dominated regime. Different results were noticed for the mixed and forced convection-dominated regimes. Thus, the inclination angles of magnetic field of $\gamma = 90°$ and $\gamma = 270°$ lead to a smaller total entropy generation, while inclination angles of $\gamma = 135°$ and $\gamma = 315°$ result in a larger total entropy generation.

The effects of magnetic field and radiation on entropy generation of Al_2O_3-water nanofluid in an inclined square cavity equipped with a conductor fin were investigated by Alnaqi et al. [56]. The fin with a thermal conductivity coefficient of $k^* = 100$ is located on one of the walls of the cavity. Fig. 15 depicts a schematic of the problem.considered by Alnaqi. The results showed that an increase in the volume concentration of nanoparticles leads to increase of total entropy generation and also, the authors concluded that the total entropy generation increases with increasing in the radiation parameter at high Rayleigh numbers and decreases at lower Rayleigh numbers.

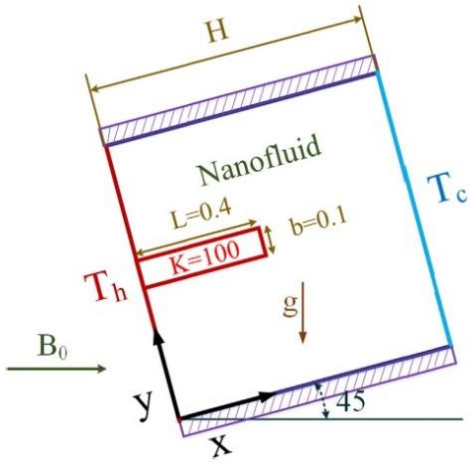

Fig. 15. The schematic of the problem considered by Alnaqi et al. [56]. Reprinted with permission from Elsevier.

In another work, Dutta et al. [57] investigated the entropy generation in a rhombic enclosure saturated with a Cu-water nanofluid under the presence of a horizontally applied magnetic field. Numerical simulations were performed for a range of Rayleigh number, $Ra = 10^3 - 10^6$, Hartmann number, $Ha = 0 - 100$, the volume concentration of nanoparticles, $\phi = 1.0 - 5.0\%$, and inclination angles of the enclosure, $\varepsilon = 30 - 60°$. They revealed that the entropy generation rate decreases with the increase in Hartmann number for all values of Rayleigh number and inclination angles of the enclosure.

Table 3 provides a summary of studies conducted on entropy generation in cavities using nanofluid.

Table 3. Summary of works done on entropy generation in cavities using nanofluid

Reference /Year	*Type of cavity*	*Nanofluid type and volume concentration*	*Method/ Model*	*Remarks*
Kefayati [40]/2016	Porous	Cu-water $\phi \leq 4.0\%$	Finite Difference Lattice Boltzmann Method / The Brinkman extended Darcy model	The increase of nanofluid volume fraction leads to increasing entropy generation at different Rayleigh numbers, power-law indexes, and Darcy numbers.
Kefayati [41]/2017	Porous	Non-Newtonian shear-thinning nanofluid	Finite Difference Lattice Boltzmann Method/ The Buongiorno's mathematical model	The entropy generation due to fluid friction was significantly affected against power-law index compared to the entropy generation due to heat and mass transfer. The increase in Darcy, Lewis, Buoyancy ratio numbers leads to increasing total entropy generation, while the total entropy generation has a different trend with increasing the Brownian motion and Thermophoresis parameters.
Hoseinpour et al. [42] /2016	Porous	Cu-water $\phi \leq 5.0\%$	Lattice Boltzmann Method	It is possible to minimize the entropy generation in the system if the porosity of the medium is varied. The entropy generation is a decreasing function of the nanofluid volume fractions.

Siavashi et al. [43] /2018	Porous	Cu-water $\phi \leq 4.0\%$	Darcy–Brinkman–Forchheimer model	The entropy generation decreases by increasing the number of fins.
Goqo et al. [44]/2019	Porous	Nanofluid-saturated porous medium	Darcy-Boussinesq model	An increase in Rayleigh number leads to the increase entropy generation when there is particle Brownian motion and that the total entropy generation reduces as the radiation parameter increases for various Hartman number values
Baghsaz et al. [45] /2019	Porous	Al_2O_3-water $\phi = 2.5\ wt\%$	In-house solver	Total entropy generation is small inside low-permeability cavity.
Malik and Nayak [46]/2017	Porous	Cu-water $\phi \leq 20.0\%$	Finite volume method / Darcy-Brinkman-Forchheimer model	The total entropy generation increases with increasing volume fraction for all studied Da numbers. The optimum value for minimum entropy generation is obtained at $Da = 0.001$ and $\phi = 0.2$ for $Gr = 10^6$ and $Ha = 50$.
Ghasemi and Siavashi [47]/2017	Porous	Cu-water $\phi \leq 12.0\%$	Lattice Boltzmann method	The minimum and the maximum total entropy generation were noticed at Ha $= 10$ and Ha $= 15$ respectively. Also, the thermal and frictional entropy generation terms were dominant for Ra $= 10^3$ and Ra $= 10^5$, respectively, while for Ra $= 10^4$ all the frictional, thermal and magnetic irreversibility terms have the same order of magnitude.
Fersadou et al. [48] /2015	Porous	Cu-water $\phi \leq 10.0\%$	Finite volume method/ Darcy–Brinkman–Forchheimer model with the Boussinesq approximation	The higher rates of entropy generation are due to friction and the rise of the volume fraction.
Hussain et al. [49] /2018	Porous	Al_2O_3-water $\phi = 4.0$ %	Monolithic Galerkin finite element method	The entropy generations due to the heat transfer and fluid friction increases with an augmentation in volume fraction, whereas entropy generation due to solutal concentration decreases with an enhancement in volume fraction.
Mahmoudi et al. [33]/2014	Square	Al_2O_3-water $\phi = 6.0$ %	Lattice Boltzmann method	Adding nanoparticle reduces the entropy generation.
Mehrez et al. [50]/2015	Open	Cu-water $\phi \leq 6.0\%$	-	At $\gamma = 0°$ (horizontal magnetic field), the entropy generation decreases by increasing both the Hartmann number (due to the attenuation of the flow intensity) and volume fraction. At $\gamma = 45°$ and $\gamma = 90°$ the

				entropy generation significantly increases by the intensification of the magnetic field and the increasing both the Hartmann number and volume fraction.
Aghaei et al. [51]/2016	Trapezoidal	Cu-water $\phi \leq 4.0\%$	Finite volume method and SIMPLER algorithm	For all Reynolds numbers and volume fractions with augmentation Hartmann number, the total entropy generation decreases.
Hussain et al. [52] /2016	Double lid driven	Al_2O_3-water $\phi = 20.0\ \%$	Galerkin weighted residual finite element method	The total entropy generation increases with an increase in Reynolds number and volume fraction.
Sheikholeslami and Ganji [53]/2015	Rectangular	Cu-water $\phi \leq 4.0\%$	Lattice Boltzmann Method	The dimensionless entropy generation number increase with increasing Rayleigh number and nanoparticle volume fraction but it decreases with increasing Hartmann number
Cho [54]/2016	Cavity with complex-wavy surfaces	Cu-water $\phi \leq 4.0\%$	The finite-volume method	Minimum total entropy generation can be noticed at a given appropriate wavelength of the wavy surface.
Alnaqi et al. [56]/2019	Inclined square	Al_2O_3-water $\phi = 6.0\ \%$	Control volume method	An increase in the volume concentration of nanoparticles leads to increase of total entropy generation. The total entropy generation increases with increasing in the radiation parameter at high Rayleigh numbers and decreases at lower Rayleigh numbers.
Dutta et al. [57]/2019	Rhombic	Cu-water $\phi \leq 5.0\%$	Rayleigh-Benard convection	The entropy generation rate decreases with the increase in Hartmann number for all values of Rayleigh number and inclination angles of the enclosure.

2.3.3. Entropy generation of natural convection in nanofluid filled cavities

Sheikholeslami et al. [58] applied the Lattice Boltzmann Method to study nanofluid flow, heat transfer, and entropy generations in a square enclosure containing a rectangular heated body. Water-based nanofluid containing different types of metal and metal-oxide nanoparticles, Al_2O_3, Cu, Ag and TiO_2, were used in cavity. The rectangular body was placed in the center of the square enclosure and is assumed to be isothermal at a comparatively higher temperature compared to the two vertical isothermal walls. Also, in this study, the top and bottom walls were

considered insulated. The results indicated that the dimensionless entropy generation number increases with both increasing Rayleigh number and volume fraction of the nanoparticles, while it decreases with increasing the ratio between the width of the cavity, H and the height of the body t, H/t.

Salari et al. [59] performed a numerical study on the entropy generation within tilted rectangular enclosures filled with stratified fluids of MWCNTs/water nanofluid and air. The main parameters involved in the problem were Rayleigh number, $Ra = 10^3 - 10^6$, solid volume fraction, $\phi = 0.002 - 0.01$, and tilt angle, $\theta = 0 - 60°$. The finite volume method was employed for computation. Fig. 16 shows a schematic of the geometry.

The 3D entropy generation equation is defined as:

$$\dot{S}_{gen} = \left\{\frac{k_{nf}}{T_0^2}\left[\left(\frac{\partial T'}{\partial x'}\right)^2 + \left(\frac{\partial T'}{\partial y'}\right)^2 + \left(\frac{\partial T'}{\partial z'}\right)^2\right]\right\} + \frac{\mu_{nf}}{T_0}\left\{2\left[\left(\frac{\partial V_x'}{\partial x'}\right)^2 + \left(\frac{\partial V_y'}{\partial y'}\right)^2 + \left(\frac{\partial V_z'}{\partial z'}\right)^2\right] + \left(\frac{\partial V_y'}{\partial x'} + \frac{\partial V_x'}{\partial y'}\right)^2 + \left(\frac{\partial V_z'}{\partial y'} + \frac{\partial V_y'}{\partial z'}\right)^2 + \left(\frac{\partial V_x'}{\partial z'} + \frac{\partial V_z'}{\partial x'}\right)^2\right\} \quad (40)$$

The total volumetric entropy generation increases with the increase of Rayleigh number. Moreover, adding of the nanoparticles in the base fluid leads to a lower entropy generation in the enclosures with different tilt angle.

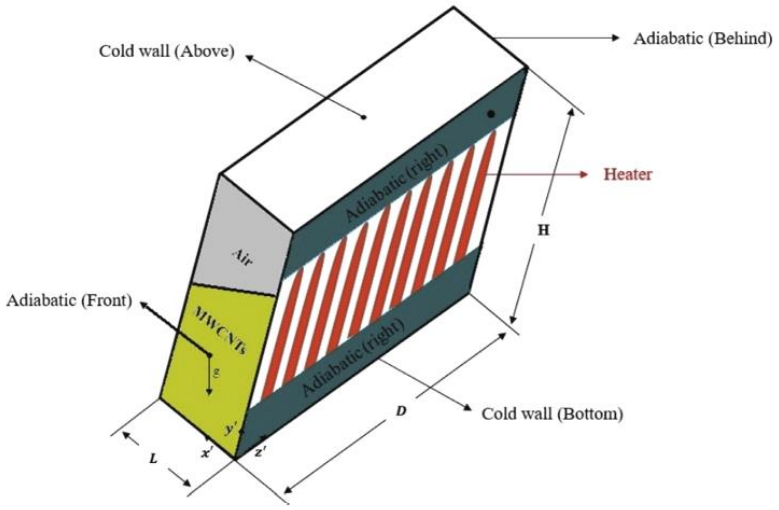

Fig. 16. The schematic of the considered problem by Salari et al. [59]. Reprinted with permission from Elsevier.

In the same year, Salari et al. [60] carried out a 3D investigation of natural convection and entropy generations within cuboids enclosure filled with two immiscible fluids, air and MWCNTs- water nanofluid. They showed that the nanofluid interface aspect ratio has significant effect on local fluid friction and heat transfer entropy generations. Thus, the results indicated that, the total entropy generation decreases with the increase of aspect ratio. The total entropy generation decreases also with increasing both of solid volume friction and Rayleigh number.

The entropy generation in Al_2O_3-water nanofluid filled cavity with thick bottom wall considering the effects of sinusoidal heating was numerical investigated by Bouchoucha et al. [61]. The bottom wall of the cavity was heated and cooled with a sinusoidal function, while the top wall was cooled isothermally. The vertical walls were considered adiabatic. The simulations were carried out for Rayleigh numbers, $Ra = 10^4 - 10^6$, solid volume fraction of 0.1, and thickness of the bottom wall $\square^* = 0.05 - 0.15$. The entropy generation due to heat transfer increases linearly with increasing of the volume fraction of nanoparticles, while the entropy generation due to viscous effects decreases with increasing of volume fraction of nanoparticles. Also, the total

entropy generation increases with increasing both Rayleigh number and volume fraction due to augmentation in the heat transfer and fluid friction irreversibility, while the increase of the wall thickness leads to reduce the total entropy generation for all studied cases.

Kefayati and Sidik [62] studied the entropy generation into natural convection of non-Newtonian nanofluid, using the Buongiorno's mathematical model in an inclined cavity. Finite Difference Lattice Boltzmann method was used to solve of the governing equations.

The main findings of this work can be summarized as follows:

- the increase of Rayleigh number augments the total irreversibility significantly in various inclined angles and power-law indexes;
- the total entropy generation increases with increasing both Lewis and Buoyancy ratio numbers;
- the total entropy generation increases as the Brownian motion and Thermophoresis parameters augment.

Bezi et al. [63] studied the entropy generation due to unsteady natural convection in a semi-annular cavity filled with nanofluid. The cavity is composed by two horizontal semiconcentric cylinders. Water-based nanofluid containing various types of nanoparticles of Au, Ag, Cu and CuO were used as working fluids. They concluded that the total entropy generation increases by increasing of volume fraction and decreases by increasing of Rayleigh number. Also, a decreasing tend in the evolution of total entropy generation depending on volume fraction is noticed for all the inclination angles γ and all aspect ratio (RR), excepting $RR = 3$ and

135°≤∝≤180°, where the average value of the total entropy generation increases with increasing volume fraction (Fig. 17).

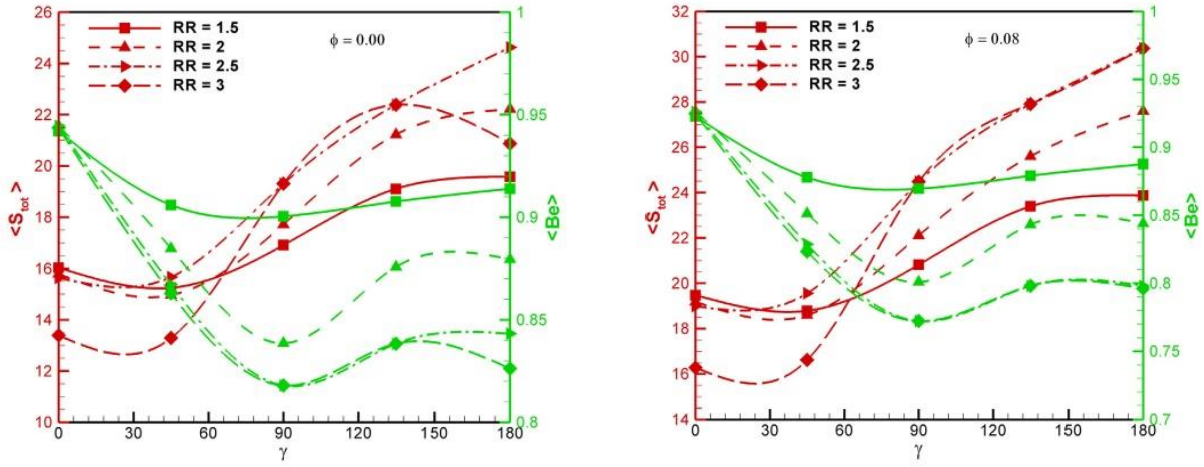

a) b)

Fig. 17. Variation in the total entropy generation with both the inclination angle and the aspect ratio for the case of base fluid (a) and CuO-water nanofluid (b) at $Ra = 10^5$ [63]. Reprinted with permission from Elsevier.

The entropy generation analysis of nanofluids thermocapillary convection around a bubble in a cavity was carried out by Jiang and Zhou [64]. The authors concluded that by adding nanoparticles in the base fluid, the local entropy generation is decreased, while a larger nanoparticles diameter leads to the increase of the total entropy generation.

In another work, Zhou et al. [65] numerical investigated the entropy generation of natural convection in a cavity using nano liquid-metal fluid, *Ga*, with different nanoparticles (copper, diamond, and carbon nanotubes). They found that the total entropy generation increases with increasing of Grashof number and nanoparticles volume fraction. The minimum and maximum entropy generations were noticed in the case Cu-Ga and CNT–Ga respectively.

2.3.4. Entropy generation due to mixed convection in nanofluid filled lid-driven cavities

Mamourian et al. [66] used the Taguchi method to optimize the mixed convection heat transfer performance and entropy generation rate in a wavy-surface square lid-driven cavity filled with Cu-water nanofluid. They found that for a given Richardson number, the entropy generation rate decrease with increasing the wavelength of the wavy surface.

The effects of the wavy fluid-solid interface, solid-to-fluid thermal conductivity ratio and nanoparticle volume fraction on the entropy generation nanofluid in a lid-driven enclosure for different of the Richardson numbers were numerical investigated by Pal et al. [67]. As working fluid Cu-water nanofluid was chosen.

The local entropy generation, $\dot{S}_{gen,l} = \dot{S}_{HT,l} + \dot{S}_{FF,l}$, in the nondimensional form, is defined as:

$$\dot{S}_{gen} = \frac{k_{nf}}{k_f}\left[\left(\frac{\partial\theta}{\partial\xi} - \frac{\eta}{g(\xi)}\,g'(\xi)\frac{\partial\theta}{\partial\eta}\right)^2\right] + \chi\frac{\mu_{nf}}{\mu_f}\left\{2\left[\left(\frac{\partial u}{\partial\xi} - \frac{\eta}{g(\xi)}g'(\xi)\frac{\partial u}{\partial\eta}\right)^2 + \left(\frac{1}{g(\xi)}\frac{\partial v}{\partial\eta}\right)^2\right] + \left[\left(\frac{1}{g(\xi)}\frac{\partial u}{\partial\eta}\right) + \left(\frac{\partial v}{\partial\xi} - \frac{\eta}{g(\xi)}g'(\xi)\frac{\partial v}{\partial\eta}\right)\right]^2\right\} \quad (41)$$

where $\chi = \frac{\mu_f\, T_0\, U_0^2}{k_f\,(T_h - T_c)}$ is the irreversibility distribution ratio, $T_0 = \frac{T_h + T_f}{2}$ is the reference temperature.

They found that:

- increase in nanoparticle volume fraction leads to increasing of total entropy generation;
- the entropy generation decreases with increasing of conductivity ratio when the fluid has higher conductivity than the wall and attains a local minimum for conductivity ratio close to 1;

- the increase both of solid conductivity and Reynolds number leads to the increase in entropy generation;
- the total entropy generation increases with increasing of amplitude or wave length of the wavy solid-fluid interface.

A similar work was performed by Gibanov et al. [68]. They numerical investigated the effects of Richardson number, bottom solid wall thickness, thermal conductivity ratio, and nanoparticles volume fraction on entropy generation in a lid-driven cavity filled with an alumina–water nanofluid.

They concluded that the average entropy generation decreases with increasing both of Richardson number and solid wall thickness and it increases with increasing both of thermal conductivity ratio and nanoparticles volume fraction.

In other work, Nayak et al. [69, 70] also investigated the entropy generation of Cu-water nanofluid in a lid-driven square cavity, and showed that the entropy generation rate increased with increasing of volume fraction of nanoparticles.

The entropy generation analysis of a lid-driven wavy wall cavity filled with Cu-water nanofluid was performed by Cho [71]. In this study, the left wall of the cavity has a flat surface and a constant high temperature, while the right wall has a wavy surface and a constant low temperature. In plus, the left wall moves in the vertical direction, the right wall remains stationary, while the upper and lower walls are both flat and insulated. The results showed that the total entropy generation increase as the Richardson number, nanoparticle volume fraction and

Reynolds number increases. This is due to a larger temperature gradient, the higher heat transfer and fluid friction irreversibilities and also a stronger convection effect. Also, the total entropy generation increase as the amplitude of the wavy surface increases for all studied Richardson numbers.

3. Entropy generation due to hybrid nanofluid flow and heat transfer

The hybrid nanofluids are new nanofluids prepared by suspending two or more nanoparticles either in a mixture or composite form, in the order improvement of heat transfer. Ahammed et al. [72] conducted an experimentally study on entropy generation of hybrid nanofluid in a two pass multiport minichannel heat exchanger coupled with a thermoelectric cooler. Alumina, graphene, and hybrid nanofluids were tested. The experiments were performed in laminar flow for the Reynolds numbers within the range 200-1000 and the heat fluxes between $6250\ \mathrm{W/m^2} - 25{,}000\ \mathrm{W/m^2}$. They concluded that the total entropy generation decreases approximately 20% with the increase in Reynolds number when the current supplied to the thermoelectric cooler and heat load were kept constant at 4A and 40W respectively.

In another work, Hussain et al. [73] numerical studied the entropy generation of Al_2O_3 –Cu/water hybrid nanofluid in a horizontal channel with an open cavity and also containing an adiabatic square obstacle inside. The schematic diagram of the considered model is shown in Fig. 18. The governing equations were solved with the Galerkin finite element method in space and the Crank-Nicolson in time.

The main findings of this work can be summarized as follows:

- the entropy generation due to heat transfer irreversibly decreases, and the entropy generations due to both fluid friction and magnetic force irreversibilities increase with the increase in the Hartmann number, but finally, the total entropy generation decreases with increasing the Hartmann and Richardson numbers.

- the increase in both the Reynolds number and nanoparticle volume fraction leads to the increase in total entropy generation.

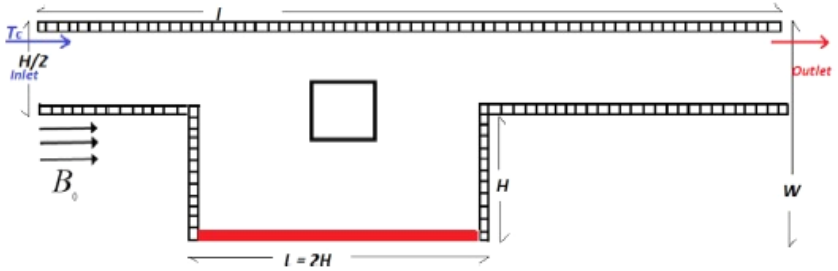

Fig. 18. The schematic of the considered problem by Hussain et al. [73]. Reprinted with permission from Elsevier.

A similar study was performed by Rahimi et al. [74]. They numerical investigated the entropy generation visualization in an H-shaped cavity filled with SiO_2-TiO_2/Water-Ethylene glycol (60:40) nanofluid with square internal bodies using lattice Boltzmann method. With the increase in volume fraction, the total entropy generation decreases due to weaker velocity magnitude of nanofluid stream and reduction in the temperature gradient. Also, the results indicated that the arrangements of internal active bodies influence the local entropy generation values.

The entropy generation analysis of MWCNT-MgO/water hybrid nanofluid in a cavity with refrigerant solid body was numerical investigated by Kasaeipoor et al. [75]. The Lattice Boltzmann method to solve of the governing equations was used. In this paper, the height of the rigid body was set at a constant value (t), and the width of the inner rigid body (w) was

considered variable. The result showed that the total entropy generation increases with increasing the Rayleigh number and it is reducing with the increase in the volume fraction of nanoparticles due to weaker velocity magnitude of nanofluid stream and reduction in the temperature gradient. Also, the numerical data showed that the ratio of t/w significant influence the total entropy generation (Fig. 19). This is attributed to larger area of cold surface increasing the transferred heat flux from side hot walls and cold rigid body.

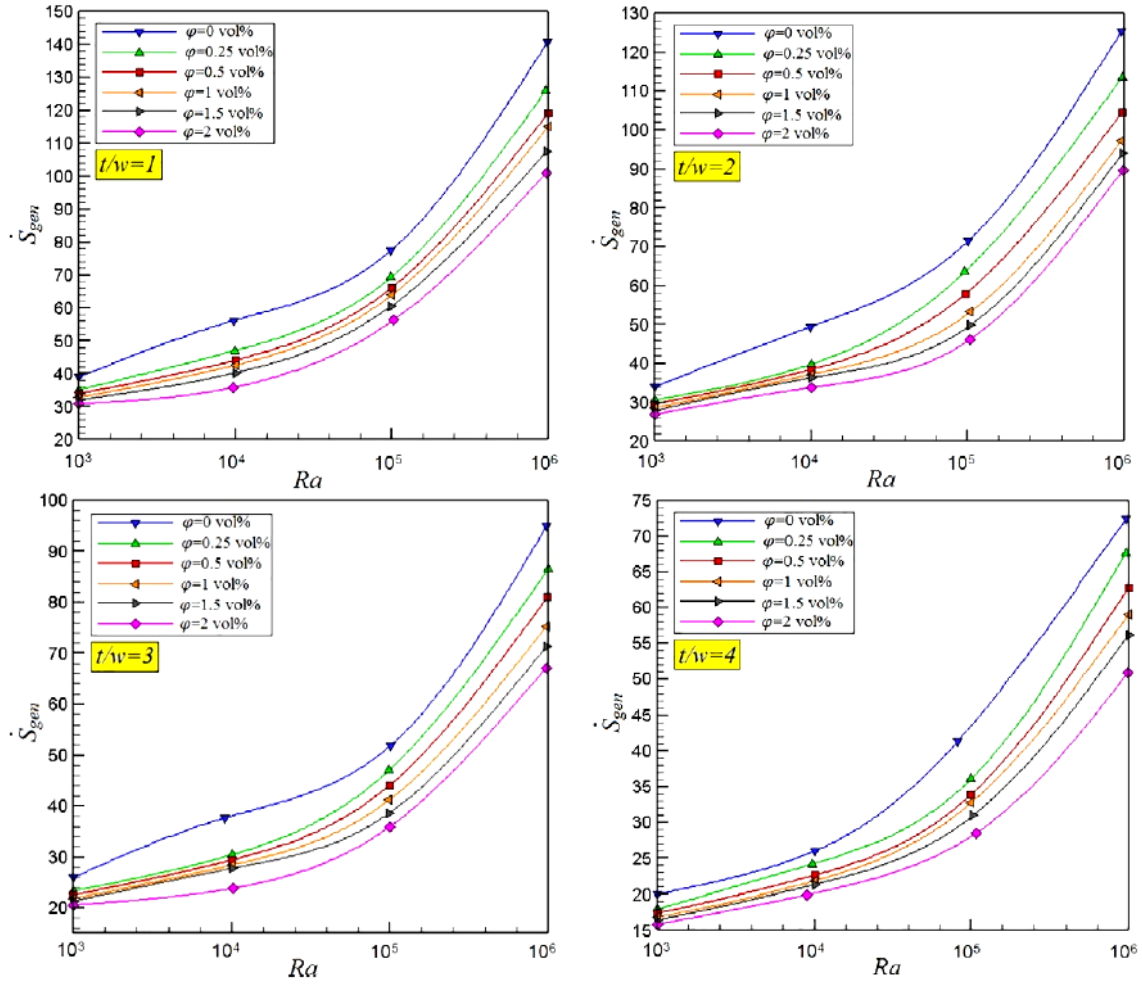

Fig. 19. Total entropy generation with respect to Rayleigh number as a function of solid volume fraction for different configurations of refrigerant rigid bodies [75]. Reprinted with permission from Elsevier.

Mehrali et al. [76] experimental studied the effects of a permanent magnetic field, the arrangement and number of magnets on the entropy generation of the graphene-Fe_3O_4/water

hybrid nanofluid flowing through a heated tube. It was found that the thermal entropy generation decreases with applying a magnetic field and the increase in velocity, while and fluid friction entropy generation decreases with applying a magnetic field but it increases with increasing velocity. The total entropy generation decreases with applying a magnetic field and it decreases with increasing velocity similar to the thermal entropy generation (Fig. 20), the reduction in the total entropy generation rate being up to 41% compared to the base fluid.

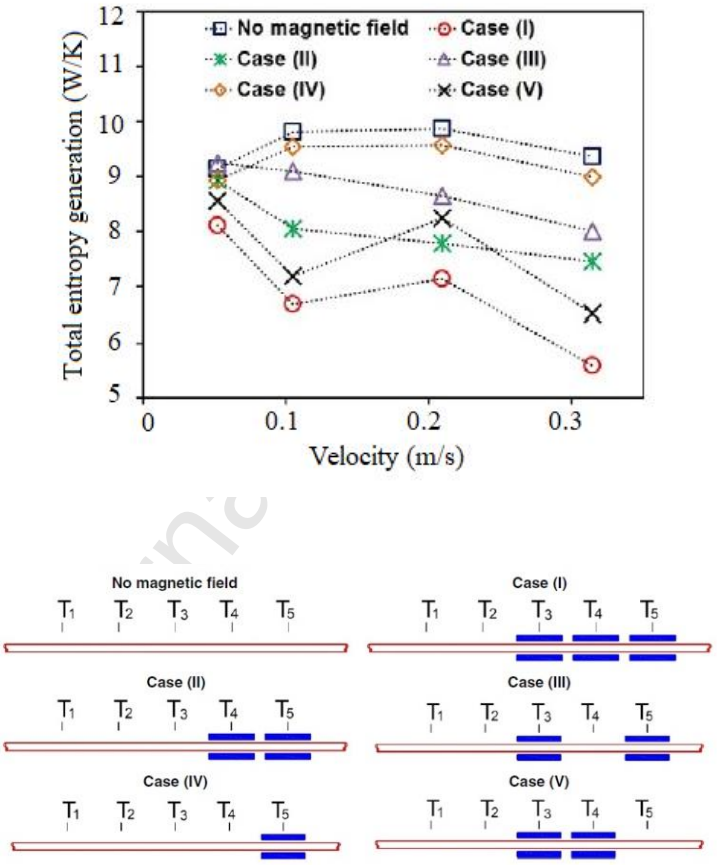

Fig. 20. Total entropy generation of rGO-Fe_3O_4 hybrid nanofluid as a function of velocity [76]. Reprinted with permission from Elsevier.

A lot of researches on entropy generation in various thermal systems were carried out by Bahiraei and Shahsavar and their team [77-84]. Bahiraei et al. [77] presented a numerical

investigation on entropy generation of a non-Newtonian hybrid nanofluid containing coated CNT/ Fe_3O_4 nanoparticles in a minichannel heat exchanger. The hybrid nanofluid flows inside the tube side, and water flows in the annulus side.The simulations were performed in laminar flow for Reynolds numbers of 500–2000, Fe_3O_4 concentrations of 0.1–0.9%, and CNT concentrations of 0–1.35%. The results revealed that the total entropy generation rate with respect to CNT concentration has a minimum value at low Fe_3O_4 concentration, while there is an ascending trend for it at high Fe_3O_4concentrations.

In a similar study, Shahsavar et al. [78] numerical studied the effect of nanoparticle volume concentration and Reynolds number on entropy generation of a hybrid nanofluid containing tetramethylammonium hydroxide (TMAH) coated Fe_3O_4 (magnetite) nanoparticles and gum arabic (GA) coated carbon nanotubes (CNTs) flowing inside a counter-flow double-pipe heat exchanger. They found that the entropy generation rate augments with increasing Reynolds number, CNT concentration, and magnetite concentration.

One year later, Shahsavar et al. [79] numerical investigated the influence of magnetic field strength, the number of dipoles and their arrangement on the entropy generation of the Mn-Zn hybrid nanofluid flowing between parallel plates. They found that the total entropy generation rate decreases with increasing magnetic field strength, number of dipoles and Reynolds number. Also, they concluded that for a single dipole its location does not influence the global total entropy generation rate, the significant changes in entropy generation variation occur when using two and three dipoles.

In another work, Shahsavar et al. [80] performed an analysis about the impacts of nanoparticle concentration and radius ratio on entropy generation of the non-Newtonian Fe_3O_4-CNT/ water hybrid nanofluid flowing inside a concentric annulus. Genetic algorithm to achieve optimal cases with maximum heat transfer and minimum entropy generation was employed. They noticed that an increase of Fe_3O_4 and CNT concentrations leads to the decrease in the global thermal entropy generation and the increase in the global frictional entropy generation and also that the contribution of the flow friction irreversibility was more than that of the heat transfer in the total entropy generation. Plus, the results indicated that augmenting the radius ratio intensifies the thermal, frictional and total entropy generation rates.

Bahiraei and Heshmatian [81] investigated the entropy generation of graphene–silver hybrid nanofluid in various liquid blocks for cooling of electronic processors. Their results indicated that the overall irreversibility was reduced due to the great thermal conductivity of graphene.

Bahiraei and Mazaheri [82] performed a numerical investigation on the entropy generation due to flow of the hybrid nanofluid containing graphene–platinum nanoparticles inside a chaotic twisted minichannel. They concluded that the thermal entropy generation decreases and frictional entropy generation increases with increasing nanoparticle concentration. Also, it was reported that due to the dominance of thermal entropy generation, the overall irreversibility of the nanofluid flow reduces.

In other study, Bahiraei et al. [83-84] carried out a study on entropy generation of graphene–platinum hybrid nanofluid flowing inside tubes equipped with double twisted tapes. They

analyzed the twisted tapes which include double co-twisted tapes and double counter twisted tapes with various twisted ratios and found that the double counter twisted tapes reduced the total entropy generation rate more compared to double co-twisted tapes. Thus, for double counter twisted tapes with a twisted ratio of 3, the increase in concentration from 0 to 0.1% leads to a decreasing in the global thermal entropy generation rate up to 14%, this being dominant in the total entropy generation rate.

Other studies on entropy generation of the hybrid nanofluids flowing in flat and elliptical tubes were performed by Huminic and Huminic [85-86]. Their results revealed that the increase in volume concentration of hybrid nanoparticles leads to a decrease in the total entropy generation for both types of tubes. For the flat tube, the reduction in total entropy generation was approximately 26% compared to the base fluid, at Re = 2000, while for the elliptical tube, the lowest dimensionless entropy generation values were noticed at Reynolds numbers within the range 50–250.

Mansour et al. [87] presented a numerical investigation on generation entropy of Al_2O_3-Cu/water hybrid nanofluid flowing inside square porous cavity differentially heated and cooled by heat source and sink. They found that the entropy generation decreases with increasing of Hartmann number and increases with increasing of nanoparticle volume fraction.

Kashyap and Dass [88] studied also the effect of boundary conditions on entropy generation of Al_2O_3 -Cu/water hybrid nanofluid flowing inside cavity. Schematic diagram of computational model with boundary conditions is shown Fig. 21. The results indicated that the Case 3 offers a

higher performance coefficient parameter, $\overline{Nu}/\overline{S_{tot}}$, due to the presence of lower heat transfer irreversibility, while the Case 1 gives lower performance coefficient parameter $\overline{Nu}/\overline{S_{tot}}$, due to its higher total entropy generation over the whole cavity. Also, the increase in volume concentration leads to a higher entropy generation.

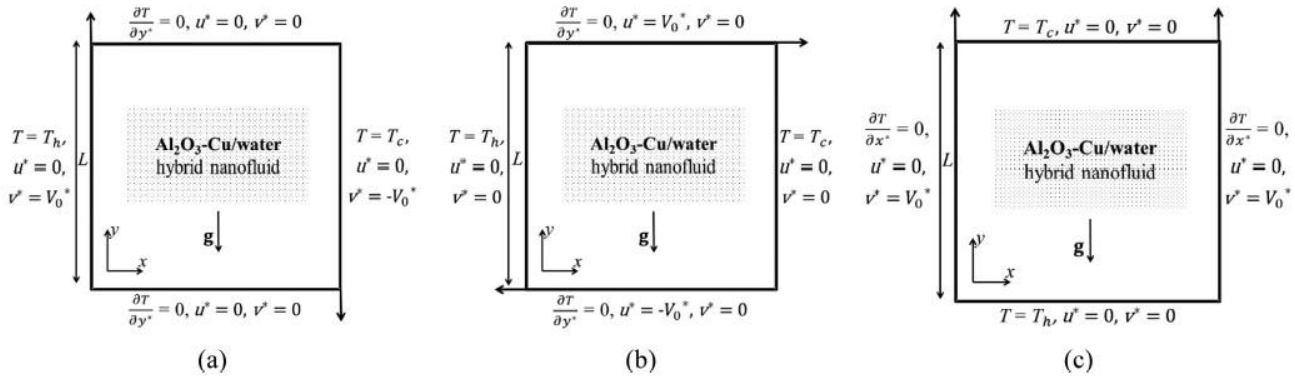

Fig. 21. Schematic of the problem [88]. Reprinted with permission from Elsevier.

Table 4 provides a summary of studies conducted on entropy generation in various thermal systems using hybrid nanofluid.

Table 4. Summary of works done on entropy generation in various thermal systems using hybrid nanofluid.

Reference /Year	*Geometry*	*Hybrid nanofluid/ volume concentration*	*Flow regime*	*Remarks*
Experimental studies				
Ahammed et al. [72]/2016	Minichannel heat exchanger	Al_2O_3-graphene/water $\phi = 0.1\%$	Laminar	The total entropy generation decreases up to 19.6%.
Mehrali et al. [76]/2017	Circular tube	Graphene-Fe3O4 /water		The total entropy generation rate was reduced up to 41% compared to distilled water.
Numerical studies				
Hussain et al. [73]/2017	Horizontal channel with	Al_2O_3- Cu /water	Laminar	The total entropy generation decreases with increasing the Hartmann, Richardson, and Reynolds numbers as

	an open cavity	$\phi \leq 4.0\%$		well as with the volume concentration of nanoparticles.
Rahimi et al. [74]/2018	H-shaped cavity	SiO_2-TiO_2 /water-EG (60:40) $\phi \leq 3.0\%$	Laminar	The total entropy generation decreases with an increase in the volume concentration of nanoparticles.
Kasaeipoor et al. [75]/2017	Cavity with refrigerant solid body	MWCNT-MgO /water $\phi \leq 0.5$ wt.%	Laminar	The total entropy generation increases with increasing the Rayleigh number and it is reducing with the increase in the volume fraction of nanoparticles.
Bahiraei et al. [77]/2017	Minichannel heat exchanger	CNT-Fe_3O_4 /water $\phi_{Fe3O4} \leq 0.9\%$ $\phi_{CNT} \leq 1.35\%$	Laminar	The total entropy generation rate with respect to CNT concentration has a minimum value at low Fe_3O_4 concentration, while there is an ascending trend for it at high Fe_3O_4 concentrations.
Shahsavar et al. [78]/2017	Counter-flow double-pipe heat exchanger	CNT-Fe_3O_4 /water	Laminar	The entropy generation rate augments with increasing Reynolds number, CNT concentration, and magnetite concentration.
Shahsavar et al. [79]/2018	Flat parallel plates	Mn-Zn/water $\phi \leq 6.0\%$	Laminar	The total entropy generation rate diminishes with the increase of magnetic field strength and Reynolds number.
Shahsavar et al. [80]/2018	Concentric annulus	CNT-Fe_3O_4 /water $\phi_{Fe3O4} \leq 0.9\%$ $\phi_{CNT} \leq 1.1\%$	Laminar	Increasing Fe_3O_4 concentration from 0.6% to 0.9% at $\phi_{CNT} = 1.1\%$ leads to 45.1% increment in the total entropy generation rates.
Bahiraei and Heshmatian [81]/2018	Microchannel heat sinks	Graphene–Ag /water $\phi \leq 0.1\%$	Laminar	The overall irreversibility was reduced due to the great thermal conductivity of graphene.
Bahiraei and Mazaheri [82]/2018	Chaotic twisted channel	Graphene–Pt /water $\phi \leq 0.1\%$	Laminar	The overall irreversibility of the nanofluid flow reduces by increasing concentration.
Bahiraei et al. [83]/2019	Tube with double twisted tapes	Graphene–Pt /water $\phi \leq 0.1\%$	Turbulent	The double counter twisted tapes reduced the total entropy generation rate more compared to double co-twisted tapes.
Bahiraei et al. [84]/2018	Micro double-pipe heat exchanger	Graphene–Ag /water $\phi \leq 0.1\%$	Laminar	Thermal entropy generation rate increases with increasing concentration, while the frictional entropy generation rate intensifies with increasing both Reynolds number and concentration.
Huminic and Huminic [85]/2018	Flat tube	MWCNT + Fe3O4 /water ND + Fe3O4 /water $\phi \leq 0.3\%$	Laminar	The MWCNT + Fe3O4/water hybrid nanofluids exhibited higher reduction in entropy generation compared to ND + Fe3O4/water hybrid nanofluids.

Huminic and Huminic [86]/2018	Elliptical tube	MgO-MWCNT /ethylene glycol $\phi \leq 0.4\%$	Laminar	The lowest dimensionless entropy generation values were noticed at Reynolds numbers within the range 50–250.
Mansour et al. [87]/2018	Square porous cavity	Al_2O_3-Cu/water $\phi \leq 0.1\%$	Laminar	The entropy generation decreases with increasing of Hartmann number and increases with increasing of nanoparticle volume fraction.
Kashyap and Dass [88]/2019	Square cavity	Al_2O_3-Cu/water $\phi \leq 3.0\%$	Laminar	The increase in volume concentration leads to a higher entropy generation.

4. Concluding remarks and future perspective

In this paper, the studies related to entropy generation of the nanofluids and hybrid nanofluids in microchannels, minichannels and cavities have been reviewed for different boundary conditions and physical situations. The reviewed literature indicates that the implementation of nanofluids/hybrid nanofluids in microchannels, minichannels and cavities may be an important alternative to the traditional thermal systems, if the main issues of those new working fluids (sedimentation, stability, high cost and production difficulties) are solved.

Based on studies reviewed, main observations can be summarized as follows:

- Microchannel:
  - The majority of the studies conducted in microchannels were numerical investigated in the laminar flow;
  - If the viscous dissipation is considered, it can be observed that there is an increase in entropy generation with increasing volume fraction;
  - The effect of streamwise conduction on the total entropy generation is significant at low-Peclet-numbers and higher nanoparticle volume concentrations;
  - The magnetic field effect is more significant than the flow friction irreversibility at the nanofluid flow through microchannel;

- Overall, studies revealed that entropy generation decreases with decreasing nanoparticle size or increasing concentration.

- The main conclusion concerning the studies conducted in the minichanels is that the total entropy generation decreases by increasing both the concentration and Reynolds number and also decreases by decreasing both the heat flux and particle size.
- Cavities:
  - the nanofluid flow is modeled using different models: the Brinkman extended Darcy model, the Buongiorno's mathematical model, the Darcy–Brinkman–Forchheimer model, and Darcy-Boussinesq model;
  - in the case of porous cavities the results showed that the increase of nanofluid volume fraction leads to increasing entropy generation at different Rayleigh numbers, power-law indexes, and Darcy numbers. Also, the total entropy generation is reduced with the radiation parameter increases for various Hartman number values;
  - for open cavities, the entropy generation decreases by increasing both the Hartmann number (due to the attenuation of the flow intensity) and volume fraction at $\gamma = 0°$ (horizontal magnetic field); application direction of magnetic field is important to minimize the entropy generation.
  - for rhombic cavities, the entropy generation rate decreases with the increase in Hartmann number for all values of Rayleigh number and inclination angles of the enclosure;

Finally, because most studies have been done numerically, further investigations are needed concerning the entropy generation analysis for the typical operating conditions of actual thermal

systems with nanofluids or hybrid nanofluids. Moreover, from the reviewed papers, it is concluded that Al_2O_3 and Cu were the most common nanoparticles used in these studies. Further studies with other types of nanoparticles are also needed.

References

[1] Kakac S, Liu H, Pramuanjaroenkij A. Heat Exchangers - Selection, Rating, and Thermal Design. CRC Press, Taylor & Francis Group; 2012.

[2] Sciacovelli A, Verda V., Sciubba E. Entropy generation analysis as a design tool—A review. Renewable Sustainable Energy Rev. 2015;43:1167–1181.

[3] Manjunath K, Kaushik SC. Second law thermodynamic study of heat exchangers: A review. Renewable Sustainable Energy Rev. 2014;40:348–374.

[4] Torabi M, Karimi N, Peterson GP, Yee S. Challenges and progress on the modelling of entropy generation in porous media: A review. Int. J. Heat Mass Transfer 2017;114:31–46.

[5] Mahian O, Kianifar A, Kleinstreuer C, Al-Nimr Moh'd A, Pop I, Sahin AZ, Wongwises S. A review of entropy generation in nanofluid flow. Int. J. Heat Mass Transfer 2013;65:514–532.

[6] Kandlikar SG, Grande WJ. Evolution of microchannel flow passages – thermohydraulic performance and fabrication technology. Heat Transfer Eng. 2003; 24:3-17

[7] Singh PK, Anoop KB, Sundararajan T, Das S K. Entropy generation due to flow and heat transfer in nanofluids. Int. J. Heat Mass Transfer 2010;53:4757–4767.

[8] Mah WH, Hung YM, Guo N. Entropy generation of viscous dissipative nanofluid flow in microchannels. Int. J. Heat Mass Transfer 2012;55:4169–4182.

[9] Bejan A. Second law analysis in heat transfer. Energy 1980;5:721-732.

[10] Ebrahimi A, Rikhtegar F, Sabaghan A, Roohi E. Heat transfer and entropy generation in a microchannel with longitudinal vortex generators using nanofluids. Energy 2016;101:190-201.

[11] Sirisha ML, Dhar P. Consequences of flow configuration and nanofluid transport on entropy generation in parallel microchannel cooling systems. Int. J. Heat Mass Transfer 2017;109:555–563.

[12] Heshmatian S, Bahiraei M. Numerical investigation of entropy generation to predict irreversibilities in nanofluid flow within a microchannel: Effects of Brownian diffusion, shear rate and viscosity gradient. Chem. Eng. Sci. 2017;172:52–65.

[13] Yue-Tzu Y, Yi-Hsien W, Bo-Ying H. Numerical optimization for nanofluid flow in microchannels using entropy generation minimization. Numer. Heat Transfer, Part A, 2015;67:571–88.

[14] Mohammadian SK, Seyf HR, Zhang Y. Performance augmentation and optimization of aluminum oxide-water nanofluid flow in a two-fluid microchannel heat exchanger. J. Heat Transfer 2014;136:02701 (9 pages).

[15] Sohel MR, Saidur R, Hassan NH, Elias MM, Khaleduzzaman SS, Mahbubul IM. Analysis of entropy generation using nanofluid flow through the circular microchannel and minichannel heat sink. Int. Commun. Heat Mass Transfer 2013;46:85–91.

[16] Manay E, Akyürek EF, Sahin B. Entropy generation of nanofluid flow in a microchannel heat sink. Results Phys. 2018;9:615–624.

[17] Alfaryjat AA, Dobrovicescu A, Stanciu D. Influence of heat flux and Reynolds number on the entropy generation for different types of nanofluids in a hexagon microchannel heat sink Chin. J. Chem. Eng. 2019;27:501–513.

[18] Al-Rashed Abdullah AAA, Shahsavar A, Entezari S, Moghimi MA, Adio SA, Nguyen TK. Numerical investigation of non-Newtonian water-CMC/CuO nanofluid flow in an offset strip-fin microchannel heat sink: Thermal performance and thermodynamic considerations. Appl. Therm. Eng. 2019;155:247–258.

[19] Ting TW, Hung YM, Guo N. Entropy generation of viscous dissipative nanofluid convection in asymmetrically heated porous microchannels with solid-phase heat generation. Energy Convers. Manage. 2015;105:731–745

[20] Ting TW, Hung YM, Guo N. Entropy generation of nanofluid flow with streamwise conduction in microchannels. Energy 2014;64:979-990.

[21] Hajialigol N, Fattahi A, Haji Ahmadi M, Ebrahim Qomi M, Kakoli E. MHD mixed convection and entropy generation in a 3-D microchannel using Al2O3–water nanofluid. J. Taiwan Inst. Chem. Eng. 2015;46:30–42.

[22] Hosseini SR, Sheikholeslami M. Investigation of the nanofluid convective flow and entropy generation within a microchannel heat sink involving magnetic field. Powder Technol. 2019;351:195–202.

[23] Hosseini SR, Ghasemian M, Sheikholeslami M, Shafee A, Li Z. Entropy analysis of nanofluid convection in a heated porous microchannel under MHD field considering solid heat generation. Powder Technol. 2019;344:914–925.

[24] Ibáñez G, López A, Pantoja J, Moreira J. Entropy generation analysis of a nanofluid flow in MHD porous microchannel with hydrodynamic slip and thermal radiation. Int. J. Heat Mass Transfer 2016;100:89–97.

[25] López A, Ibáñez G, Pantoja J, Moreira J, Lastres O. Entropy generation analysis of MHD nanofluid flow in a porous vertical microchannel with nonlinear thermal radiation, slip flow and convective-radiative boundary conditions. Int. J. Heat Mass Transfer 2017; 107:982–994.

[26] Mahian O, Kianifar A, Heris SZ, Wongwises S. First and second laws analysis of a minichannel-based solar collector using boehmite alumina nanofluids: Effects of nanoparticle shape and tube materials. Int. J. Heat Mass Transfer 2014;78:1166–1176.

[27] Mahian O, Kianifar A, Sahin AZ, Wongwises S. Performance analysis of a minichannel-based solar collector using different nanofluids. Energy Convers. Manage. 2014;88: 129–138.

[28] Bahiraei M, Abdi F. Development of a model for entropy generation of water-TiO2 nanofluid flow considering nanoparticle migration within a minichannel. Chemom. Intell. Lab. Syst. 2016;157:16–28.

[29] Bahiraei M, Majd SM. Prediction of entropy generation for nanofluid flow through a triangular minichannel using neural network. Adv. Powder Technol. 2016;27:673–683.

[30] Bahiraei M, Gharagozloo K, Alighardashi M, Mazaheri N. CFD simulation of irreversibilities for laminar flow of a power-law nanofluid within a minichannel with chaotic perturbations: An innovative energy-efficient approach. Energy Convers. Manage. 2017;144:374–387.

[31] Bahiraei M, Mazaheri N, Bakhti A. Irreversibility characteristics of nanofluid flow under chaotic advection in a minichannel for different nanoparticle types. J. Taiwan Inst. Chem. Eng. 2018;88:25–36.

[32] Al-Rashed Abdullah AAA, Ranjbarzadeh R, Aghakhani S, Soltanimehr M, Afrand M, Nguyen TK. Entropy generation of boehmite alumina nanofluid flow through a minichannel heat exchanger considering nanoparticle shape effect. Physica A 2019;521:724–736.

[33] Mahmoudi A, Mejri I, Abbassi MA, Omri A. Analysis of the entropy generation in a nanofluid-filled cavity in the presence of magnetic field and uniform heat generation/absorption. J. Mol. Liq. 2014;198:63–77.

[34] Bouchmel M, Nabil B, Ammar AM, Kamel G, Ahmed O. Entropy generation and heat transfer of Cu-water nanofluid mixed convection in a cavity. Int. J. Mech., Aerosp., Ind., Mechatron. Manuf. Eng. 2014;8:2137-2143.

[35] Nayak RK, Bhattacharyya S, Pop I. Numerical study on mixed convection and entropy generation of Cu-water nanofluid in a differentially heated skewed enclosure. Int. J. Heat Mass Transfer 2015;85:620–634.

[36] Bouchoucha AM, Bessaih R. Natural convection and entropy generation of nanofluids in a square cavity. Int. J. Heat Technol. 2015;33:1–10.

[37] Selimefendigil F, Öztop HF, Hamdeh NA. Natural convection and entropy generation in nanofluid filled entrapped trapezoidal cavities under the influence of magnetic field. Entropy 2016;18:43.

[38] Selimefendigil F, Öztop HF, Chamkha AJ. MHD mixed convection and entropy generation of nanofluid filled lid driven cavity under the influence of inclined magnetic fields imposed to its upper and lower diagonal triangular domains. J. Magn. Magn. Mater. 2016;406:266-281.

[39] Chamkha A, Ismael M, Kasaeipoor A, Armaghani T. Entropy generation and natural convection of CuO-water nanofluid in C-shaped cavity under magnetic field. Entropy 2016;18:50.

[40] Kefayati GHR. Heat transfer and entropy generation of natural convection on non-Newtonian nanofluids in a porous cavity. Powder Technol. 2016;299127–149.

[41] Kefayati GHR. Simulation of natural convection and entropy generation of non-Newtonian nanofluid in a porous cavity using Buongiorno's mathematical model. Int. J. Heat Mass Transfer 2017;112:709–744.

[42] Hoseinpour B, Ashorynejad HR, Javaherdeh K. Entropy generation of nanofluid in a porous cavity by lattice Boltzmann method. J. Thermophys Heat Transfer 2016;31:1–8.

[43] Siavashi M, Yousofvand R, Rezanejad S. Nanofluid and porous fins effect on natural convection and entropy generation of flow inside a cavity. Adv. Powder Technol. 2018;29:142–156.

[44] Goqo SP, Mondal H, Sibanda P, Motsa SS. A multivariate spectral quasilinearisation method for entropy generation in a square cavity filled with porous medium saturated by nanofluid. Case Stud. Therm. Eng. 2019;14:100415.

[45] Baghsaz S, Rezanejad S, Moghimi M. Numerical investigation of transient natural convection and entropy generation analysis in a porous cavity filled with nanofluid considering nanoparticles sedimentation. J. Mol. Liq. 2019;279:327–341.

[46] Malik S, Nayak AK. MHD convection and entropy generation of nanofluid in a porous enclosure with sinusoidal heating. Int. J. Heat Mass Transfer 2017;111: 329–345.

[47] Ghasemi K, Siavashi M. MHD nanofluid free convection and entropy generation in porous enclosures with different conductivity ratios. J. Magn. Magn. Mater. 2017;442:474–490.

[48] Fersadou I, Kahalerras H, Ganaoui ME. MHD mixed convection and entropy generation of a nanofluid in a vertical porous channel. Comput. Fluids 2015;121:164–179.

[49] Hussain S, Mehmood K, Sagheer M, Yamin M. Numerical simulation of double diffusive mixed convective nanofluid flow and entropy generation in a square porous enclosure. Int. J. Heat Mass Transfer 2018;122:1283–1297.

[50] Mehrez Z, Cafsi AE, Belghith A, Le Quéré P. MHD effects on heat transfer and entropy generation of nanofluid flow in an open cavity. J. Magn. Magn. Mater.2015;374:214–224.

[51] Aghaei A, Khorasanizadeh H, Sheikhzadeh G, Abbaszadeh M. Numerical study of magnetic field on mixed convection and entropy generation of nanofluid in a trapezoidal enclosure. J. Magn. Magn. Mater. 2016;403:133–145.

[52] Hussain S, Mehmood K, Sagheer M. MHD mixed convection and entropy generation of water alumina nanofluid flow in a double lid driven cavity with discrete heating. J. Magn. Magn. Mater. 2016;419:140–155.

[53] Sheikholeslami M, Ganji DD. Entropy generation of nanofluid in presence of magnetic field using Lattice Boltzmann Method. Physica A 2015;417:273–286.

[54] Cho CC. Influence of magnetic field on natural convection and entropy generation in Cu–water nanofluid-filled cavity with wavy surfaces. Int. J. Heat Mass Transfer2016;101:637–647.

[55] Cho CC. Mixed convection heat transfer and entropy generation of Cu-water nanofluid in wavy-wall lid-driven cavity in presence of inclined magnetic field. Int. J. Mech. Sci. 2019;151:703–714.

[56] Alnaqi AA, Aghakhani S, Pordanjani AH, Bakhtiari R, Asadi A, Tran MD. Effects of magnetic field on the convective heat transfer rate and entropy generation of a nanofluid in an inclined square cavity equipped with a conductor fin: Considering the radiation effect. Int. J. Heat Mass Transfer 2019;133:256–267.

[57] Dutta S, Goswami N, Biswas AK, Pati S. Numerical investigation of magnetohydrodynamic natural convection heat transfer and entropy generation in a rhombic enclosure filled with Cu-water nanofluid. Int. J. Heat Mass Transfer 2019;136:777–798.

[58] Sheikholeslami M, Ashorynejad HR, Rana P. Lattice Boltzmann simulation of nanofluid heat transfer enhancement and entropy generation. J. Mol. Liq. 2016;214:86–95.

[59] Salari M, Malekshah EH, Malekshah MH, Alavi M, Hajihashemi R. 3D numerical analysis of natural convection and entropy generation within tilted rectangular enclosures filled with stratified fluids of MWCNTs/water nanofluid and air. J. Taiwan Inst. Chem. Eng. 2017;80:624–638.

[60] Salari M, Malekshah EH, Esfe MH. Three dimensional simulation of natural convection and entropy generation in an air and MWCNT/water nanofluid filled cuboid as two immiscible fluids with emphasis on the nanofluid height ratio's effects. J. Mol. Liq. 2017;227: 223–233.

[61] Bouchouchaa AEM, Bessaïh R, Oztop HF, Al-Salem K, Bayrak F. Natural convection and entropy generation in a nanofluid filled cavity with thick bottom wall: Effects of non-isothermal heating. Int. J. Mech. Sci. 2017;126:95–105.

[62] Kefayati GHR, Sidik NAC. Simulation of natural convection and entropy generation of non-newtonian nanofluid in an inclined cavity using buongiorno's mathematical model (Part II, entropy generation). Powder Technol. 2017;305:679–703.

[63] Bezi S, Souayeh B, Ben-Cheikh N, Ben-Beya B. Numerical simulation of entropy generation due to unsteady natural convection in a semi-annular enclosure filled with nanofluid. Int. J. Heat Mass Transfer 2018;124:841–859.

[64] Jiang Y, Zhou X. Heat transfer and entropy generation analysis of nanofluids thermocapillary convection around a bubble in a cavity. Int. Commun. Heat Mass Transfer 2019;105:37–45.

[65] Zhou X, Jiang Y, Li X, Cheng K, Huai X, Zhang X, Huang H. Numerical investigation of heat transfer enhancement and entropy generation of natural convection in a cavity containing nano liquid-metal fluid. Int. Commun. Heat Mass Transfer 2019;106: 46–54.

[66] Mamourian M, Shirvan KM, Ellahi R, Raimi AB. Optimization of mixed convection heat transfer with entropy generation in a wavy surface square lid-driven cavity by means of Taguchi approach. Int. J. Heat Mass Transfer 2016;102:544–554.

[67] Pal SK, Bhattacharyya S, Pop I. Effect of solid-to-fluid conductivity ratio on mixed convection and entropy generation of a nanofluid in a lid-driven enclosure with a thick wavy wall. Int. J. Heat Mass Transfer 2018;127:885–900.

[68] Gibanov NS, Sheremet MA, Oztop HF, Abu-Hamdeh N. Mixed convection with entropy generation of nanofluid in a lid-driven cavity under the effects of a heat-conducting solid wall and vertical temperature gradient. Eur. J. Mech. B. Fluids 2018;70:148–159.

[69] Nayak RK, Bhattacharyya S, Pop I. Numerical study on mixed convection and entropy generation of a nanofluid in a lid-driven square enclosure. ASME J. Heat Transf. 2016;138: 012503.

[70] Nayak RK, Bhattacharyya S, Pop I. Heat transfer and entropy generation in mixed convection of a nanofluid within an inclined skewed cavity. Int. J. Heat Mass Transfer 2016;102: 596–609.

[71] Cho CC. Heat transfer and entropy generation of mixed convection flow in Cu-water nanofluid-filled lid-driven cavity with wavy surface. Int. J. Heat Mass Transfer 2018;119:163–174.

[72] Ahammed N, Asirvatham LG, Wongwises S. Entropy generation analysis of graphene–alumina hybrid nanofluid in multiport minichannel heat exchanger coupled with thermoelectric coole. Int. J. Heat Mass Transfer 2016;103:1084–1097.

[73] Hussain S, Ahmed SE, Akbar T. Entropy generation analysis in MHD mixed convection of hybrid nanofluid in an open cavity with a horizontal channel containing an adiabatic obstacle. Int. J. Heat Mass Transfer 2017;114:1054–1066.

[74] Rahimi A, Sepehr M, Lariche MJ, Mesbah M, Kasaeipoor A, Malekshah EH. Analysis of natural convection in nanofluid-filled H-shaped cavity by entropy generation and heatline visualization using lattice Boltzmann method. Physica E: Low-dimensional Systems and Nanostructures 2018;97:347–362.

[75] Kasaeipoor A, Malekshah EH, Kolsi L. Free convection heat transfer and entropy generation analysis of MWCNT-MgO (15% −85%)/Water nanofluid using Lattice Boltzmann method in cavity with refrigerant solid body-Experimental thermo-physical properties. Powder Technol. 2017;322:9–23.

[76] Mehrali M, Sadeghinezhad E, Akhiani AR, Latibari ST, Metselaar HSC, Kherbeet AS, Mehrali M. Heat transfer and entropy generation analysis of hybrid graphene/Fe3O4 ferro-nanofluid flow under the influence of a magnetic field. Powder Technol. 2017;308;149–157.

[77] Bahiraei M, Berahmand M, Shahsavar A. Irreversibility analysis for flow of a non-Newtonian hybrid nanofluid containing coated CNT/Fe3O4 nanoparticles in a minichannel heat exchanger. Appl. Therm. Eng. 2017;125:1083–1093.

[78] Shahsavar A, Rahimi Z, Bahiraei M. Optimization of irreversibility and thermal characteristics of a mini heat exchanger operated with a new hybrid nanofluid containing carbon nanotubes decorated with magnetic nanoparticles. Energy Convers. Manage. 2017;150:37–47.

[79] Shahsavar A, Ansarian R, Bahiraei M. Effect of line dipole magnetic field on entropy generation of Mn-Zn ferrite ferrofluid flowing through a minichannel using two-phase mixture model. Powder Technol. 2018;340:370–379.

[80] Shahsavar A, Moradi M, Bahiraei M. Heat transfer and entropy generation optimization for flow of a non-Newtonian hybrid nanofluid containing coated CNT/Fe3O4 nanoparticles in a concentric annulus. J. Taiwan Inst. Chem. Eng. 2018;84:28–40.

[81] Bahiraei M, Heshmatian S. Thermal performance and second law characteristics of two new microchannel heat sinks operated with hybrid nanofluid containing graphene–silver nanoparticles, Energy Convers. Manage. 2018;168:357–370.

[82] Bahiraei M, Mazaheri N. Second law analysis for flow of a nanofluid containing graphene–platinum nanoparticles in a minichannel enhanced with chaotic twisted perturbations. Chem. Eng. Res. Des. 2018;136:230–241.

[83] Bahiraei M, Mazaheri N, Aliee F. Second law analysis of a hybrid nanofluid in tubes equipped with double twisted tape inserts. Powder Technol. 2019;345:692–703.

[84] Bahiraei M, Jamshidmofid M, Amani M, Barzegarian R. Investigating exergy destruction and entropy generation for flow of a new nanofluid containing graphene–silver nanocomposite in a micro heat exchanger considering viscous dissipation. Powder Technol. 2018;336: 298–310.

[85] Huminic G, Huminic A. The heat transfer performances and entropy generation analysis of hybrid nanofluids in a flattened tube. Int. J. Heat Mass Transfer 2018;119:813–827.

[86] Huminic G, Huminic A. The influence of hybrid nanofluids on the performances of elliptical tube: Recent research and numerical study. Int. J. Heat Mass Transfer 2019;129:132–143.

[87] Mansour MA, Siddiqa S, Gorla RSR, Rashad AM. Effects of heat source and sink on entropy generation and MHD natural convection of Al2O3-Cu/water hybrid nanofluid filled with square porous cavity. Therm. Sci. Eng.Prog. 2018;6:57–71.

[88] Kashyap D, Dass AK., Effect of boundary conditions on heat transfer and entropy generation during two-phase mixed convection hybrid Al2O3-Cu/water nanofluid flow in a cavity, Int. J. Mech. Sci. 157–158 (2019) 45–59.

Graphical abstract

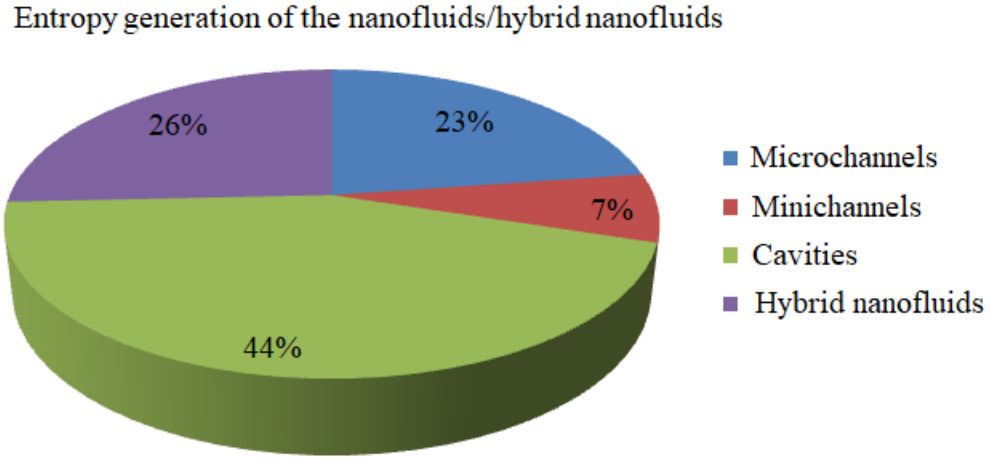

Source: ScienceDirect 2010-2019

Highlights

- ✓ This review explores potential nanofluids and hybrid nanofluids in the entropy generation minimization.
- ✓ Both numerical and experimental research is reviewed, including macro- microchannels and cavities.
- ✓ Investigations of nanofluids and hybrid nanofluids in thermal systems are summarized.